Colloids and Surfaces A: Physicochemical and Engineering Aspects 659 (2023) 130687

Contents lists available at ScienceDirect

Colloids and Surfaces A: Physicochemical and Engineering Aspects

journal homepage: www.elsevier.com/locate/colsurfa

Synthesis of Gemini cationic surfactants based on natural nicotinic acid and evaluation of their inhibition performance at C-steel/1 M HCl interface: Electrochemical and computational investigations

A. Elaraby [a,1], Amr Elgendy [a,b], M. Abd-El-Raouf [a], M.A. Migahed [a], A.S. El-Tabei [a], Aboubakr M. Abdullah [c], Noora H. Al-Qahtani [c], Sami M. Alharbi [d], Samy M. Shaban [a,e,f], Dong-Hwan Kim [e,f,*], N.M. El Basiony [a,e,f,**,1]

[a] Egyptian Petroleum Research Institute, Nasr City 11727, Cairo, Egypt
[b] Department of Chemistry and Henry Royce Institute, University of Manchester, Manchester M13 9PL, UK
[c] Center for Advanced Materials, Qatar University, P.O. Box 2713, Doha, Qatar
[d] Department of Chemistry, College of Science, Qassim University, Buraydah Almolaydah, P.O. Box 6644, Buraydah 51452, Saudi Arabia
[e] Biomedical Institute for Convergence at SKKU (BICS), Sungkyunkwan University, 16419, Republic of Kore
[f] School of Chemical Engineering, Sungkyunkwan University, Suwon 16419, Republic of Korea

HIGHLIGHTS

- Highly effective low-cost cationic surfactants are prepared.
- CS_{II} and CSIV chemical structures confirmed by FTIR.
- MCs confirmed the higher E_{ads} of CS_{IV} over CS_{II}.
- CS_{II} and CS_{IV} are mixed type inhibitors.
- CS_{II} and CS_{IV} are well-adsorbed at interfaces.

GRAPHICAL ABSTRACT

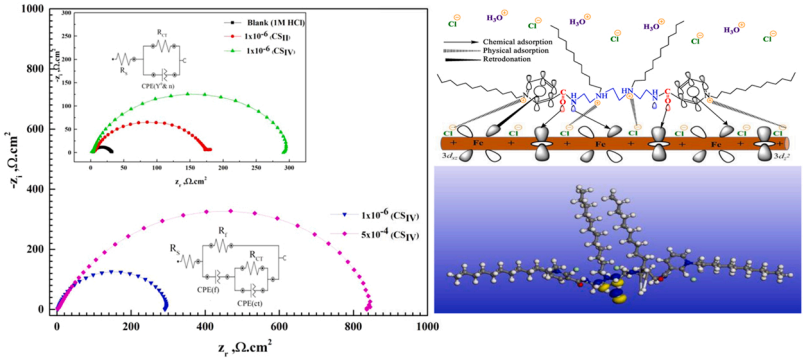

ARTICLE INFO

Keywords:
Corrosion
Adsorption
EIS
MCs
Langmuir isotherm
Surfactants

ABSTRACT

Herein, we prepare effective Gemini cationic surfactants (CS_{II}, CS_{IV}) and characterize them using FT-IR and ^{1}HNMR spectroscopy. The adsorptive properties of CS_{II} and CS_{IV} at HCl/air and C-steel/HCl interfaces were examined with surface tension and electrochemical parameters, respectively. The critical micelle concentration (CMC) of the CS_{II} and CS_{IV} indicated their adsorption affinity at the HCl/air interface. Where, aliphatic chains increase surface coverage percentage and aid in surfactant adsorption. The electrochemical parameters of C-steel in 1 M HCl were studied using electrochemical impedance spectroscopy (EIS) and potentiodynamic polarization

* Corresponding author at: Biomedical Institute for Convergence at SKKU (BICS), Sungkyunkwan University, 16419, Republic of Kore.
** Corresponding author at: School of Chemical Engineering, Sungkyunkwan University, Suwon 16419, Republic of Korea.
E-mail addresses: dhkim1@skku.edu (D. Kim), n.elbasiony@skku.edu, n.elbasiony56@gmail.com (N.M. El Basiony).
[1] The authors A. Elaraby and N.M. El Basiony contributed equally to this article.

https://doi.org/10.1016/j.colsurfa.2022.130687
Received 31 August 2022; Received in revised form 23 November 2022; Accepted 26 November 2022
Available online 1 December 2022

(PDP) at different temperatures. The charge transfer resistance of the C-steel electrode was enhanced from 28.2 Ω.cm^2 to 770.79 and 831.45 Ω.cm^2 after adding 5×10^{-4} M of CS_{II} and CS_{IV}, respectively. Both CS_{II} and CS_{IV} act as mixed inhibitors with inhibition performance exceeding 97% due to their highly adsorption affinity. The chemical adsorption affinity of these compounds is suggested by the higher adsorption energy (ΔG^*_{ads}) values (>-40 kJ mol^{-1}) according to the Langmuir isotherm model. The theoretical calculations including DFT, and Monte Carlo simulation (MCs) provide insight into the relationship between corrosion inhibition and molecular structure, where the calculated parameters agree with the experimental results.

1. Introduction

Steel is used in a variety of products, including construction, heat exchangers, boilers, railroads, and pipelines [1]. The reason for this is its low cost and its physical-mechanical characteristics [2]. However, in the oil gas industry corrosive hydrochloric acid (HCl) is commonly used to remove unwanted scales such as mill-scale from steel, rust, or any ferrous alloys as well as pickling acids for acidification jobs at higher temperatures [1,3]. In the last few years, scientists interested in finding an efficient method for the treatment and prevention of metal's corrosion. Among these techniques is the use of corrosion inhibitors (CIs), which cover the metal surface through their active groups, and reducing the reaction between the metal and its surroundings [4–6]. CIs adsorb chemically on the steel surface via donating electrons to the incompletely filled 3d orbital of iron and physically via electrostatic attraction forces between CIs' charged centers and charged metal surface [7–9]. As compared to traditional CIs, surfactants based CIs are more affordable, easy to produce, high in inhibition efficiency, and low in toxicity [10, 11]. Gemini cationic surfactants have a wide range of industrial applications including detergents, wetting agents, emulsifiers and also, corrosion inhibitors for various metals [10,12]. Gemini cationic surfactant is made up of two hydrophilic groups, and two hydrophobic groups that are linked together by a rigid and stretchy aromatic and/or an aliphatic spacer. These class of surfactants have attracted considerable interest from researchers because they are more efficient corrosion inhibitors even at a low concentration than monomeric cationic surfactants [13–17]. Abdallah et al. [18] investigated the effect of cationic Gemini surfactant (CGS) on C-steel in HCl. The results showed that CGS formed a stable adsorption layer with an inhibition potency touch of 94%. N.M. El Basiony et al. [16] investigated the corrosion potency of the prepared cationic Gemini surfactant (GI-surfactant) in HCl for X-65 steel. The inhibition efficiency increased with concentration until it reached 91.44%, then decreased with temperature reached 64.67%. Samy M. Shaban et al. [19] investigated the inhibition performance of three Gemini cationic surfactants (CMTC, LMTC, and PMTC) for C-steel in acidic solution at various temperatures. The PMTC exhibited the lowest CMC and the highest inhibition potency due to its longer alkyl fatty chain than the other tested compounds. The present study is unique in that, the synthesis of two Gemini cationic surfactants (Di & Tetra) enriched with high electron density from available and low-cost starting materials (nicotinic acid). Also, these compounds possess a high affinity to adsorb at the interface compared to the published compounds as well as the ability to resist C-steel in harsh industrial conditions such as higher temperatures and longer immersion time. Herein, we will investigate the ability of synthesized Di and Tetra cationic surfactants (CS_{II} and CS_{IV}) to suppress C-steel corrosion in 1 M HCl solutions based on EIS and PDP output results. The adsorption of these compounds have been studied using different isotherm models. For further confirmation, we also explored the surface morphology to ensure the inhibition mechanism. Finally, we investigated the affinity of the compounds tested as corrosion inhibitors based on density function theory (DFT) and MCs point of views.

2. Experimental methods

2.1. Materials sources

El-Nasr company supplied the nicotinic acid, while Sigma-Aldrich supplied the methanol, sulfuric acid, ethanol, chloroform and 1-chlorododecane. Merck supplied the Triethylentertamine. All the purchased chemicals were used without further purification.

2.2. Synthesis of Gemini cationic surfactants

According to Scheme 1, the Gemini cationic surfactants (CS_{II} and CS_{IV}) have been prepared and characterized during successive steps and discussed in detail in supporting information material.

2.3. Surface-active properties of the synthesized surfactants

Surface tension of CS_{II} and CS_{IV} in 1 M HCl at 20 °C ± 1 °C measured using Tensiometer-K6-Germany based on the platinum ring method. After each run, the Pt ring was cleaned with acetone and di-distilled water. Some surface parameters were calculated, including effectiveness (π_{CMC}), maximum surface excess (Γ_{max}), and minimum surface area (A_{min}).

2.4. Solutions

CS_{II} and CS_{IV} concentration series were prepared by building their stock solutions (1×10^{-2} M) in 1 M HCl via dilution at 20 °C ± 1 °C.

2.5. Electrochemical measurement (EMs)

The three-electrode system connected to the PGSTAT 128 n Galvanostat/ potentiostat instrument, consisted of the C-steel with chemical composition in wt%; (Cr: 0.015, P: 0.005, Mn: 0.751, Si: 0.058, C: 0.078, and Fe balanced) set as working electrode, Ag/AgCl (3 M KCl) as reference electrode, and platinum wire as auxiliary electrode. Before each run, the C-steel electrode was polished with emery papers of varying grades (600–2500). After immersing the C-steel electrode for 30 min, EIS and PDP measurements were performed. This period is sufficient to determine the steady-state potential of the C-steel in the absence and presence of inhibitors and presented in Fig. Si 7 [26–29]. EIS measurements were measured within a frequency range from 100 kHz to 0.05 Hz at 5 mv amplitude. PDP measured within a potential range of ± 400 mV around the open circuit potential (OCP) at a scan rate of 1 mV/s. The thermodynamic parameters of C-steel reaction in HCl with and without 5×10^{-4} M from the tested compounds were determined using EMs at various temperatures. The mean values of the repeated experiments were recorded. The uncertainty values for the charge transfer resistance (R_{ct}) and those of corrosion current density (I_{corr}) have been calculated and reported in Table Si 2.

2.6. Surface analysis

C-steel sheets (1 ×1 cm) were soaked in 1 M HCl treated and untreated with 5×10^{-4} M CS_{IV} as a representative optimum concentration of the best used corrosion inhibitors. Surface analysis study was carried

out after 6 h of immersion using QUANTA FEG 250 scanning electron microscope with accelerating voltage of 20 kV and magnification power 4000 X [16,24]. Elemental analysis of the outer layer surface of the C-steel was examined using an energy-dispersive X-ray spectroscopy (EDX) unit attached to SEM.

2.7. Theoretical quantum chemical study

Frontier molecular orbitals (FMO) of CS_{II} and CS_{IV} in the gas phase were obtained using the VAMP module included in Material studio software (Ms 6.0). VAMP geometry optimization process with convergence tolerance criteria of medium quality and 0.4 Kcal/mol/A Gradient using NDDO with PM3. The electronic optimization of VAMP is followed by the standard convergence scheme. SCF tolerance $1e^{-5}$ with maximum cycle 200 and medium quality. The FMO of CS_{II} and CS_{IV}, as well as their relevant energies, were discussed to shed the light on the ability of CS_{II} and CS_{IV} compounds to act as C-steel inactivators. Furthermore, the interaction between CS_{II} and CS_{IV} compounds and iron surface was simulated based on MCs method using adsorption locator module implemented in MS 6.0. MCs. The simulations were performed in a vacuum and simulated acidic environment (100 H_2O + 5 H_3O^+ + 5Cl^-) to simulate the corrosion conditions. To obtain the adsorption energy parameters, MCs were carried out by loading the optimized structures of CS_{II} and CS_{IV} separately over the most stable plan of iron Fe (110). The setting parameters of MCs were previously stated in our previous work [16].

3. Results and discussion

3.1. Surface active parameters study

Surface tension measurements were used to investigate the surface-active properties of the prepared CS_{II} and CS_{IV} surfactants. Adsorption of CS_{II} and CS_{IV} unimer at the 1 M HCl solution/air interface reduces HCl solution surface tension. Fig. 1 depicts the relationship between surface tension (γ) and the concentration of the studied surfactants (-log C). The surface tension of 1.0 M HCl solution gradually decreased as the concentration of CS_{II} and CS_{IV} increased till saturation point where there is no more detectable change in the surface tension. That saturation point, known as CMC at which the CS_{II} and CS_{IV} unimer aggregates constructing a micelle structure in bulk, where no significant changes have been observed for the surface tension. The calculated CMCs values in Table Si 1, correspond to the intersection between premicellar and post micellar lines [25,26], and revealed that the CS_{II} cationic surfactant with two hydrophobic tails has a low value of CMC (6.25×10^{-4} M) compared to the CS_{IV} cationic surfactant (1.25×10^{-3} M) which has four hydrocarbon tails reflecting the effect of the hydrophobic tail on the CMC values. Increasing the number of the surfactant hydrophobic tails render system more hydrophobic and thus increasing the system free energy because of destroying the water structure. Based on that the affinity of the CS_{IV} surfactant to migrate and adsorb on the surface or aggregate and constructing micelle is higher [27,28]. So, the increasing

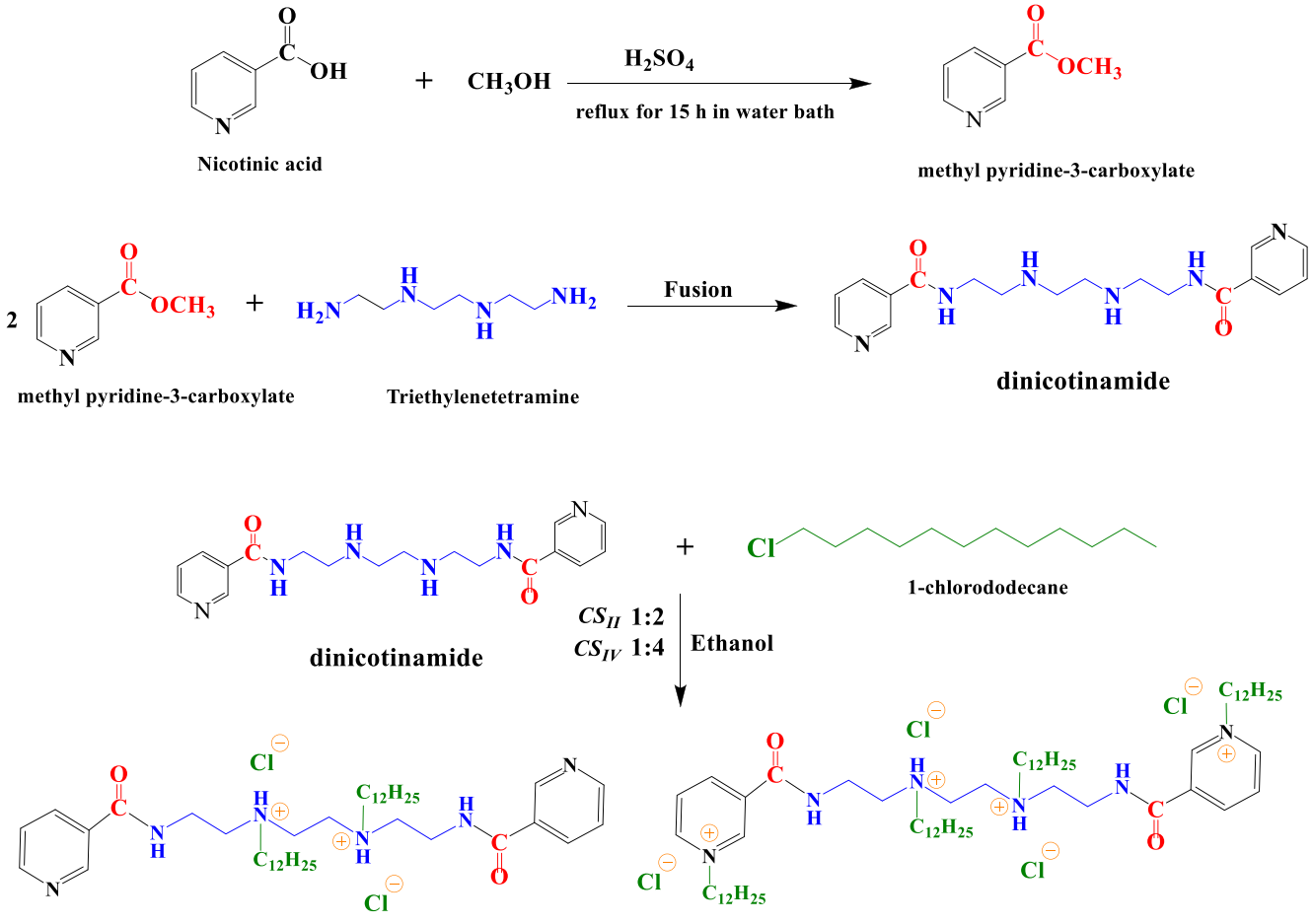

Scheme1. Synthesis of CS_{II} and CS_{IV} cationic surfactants.

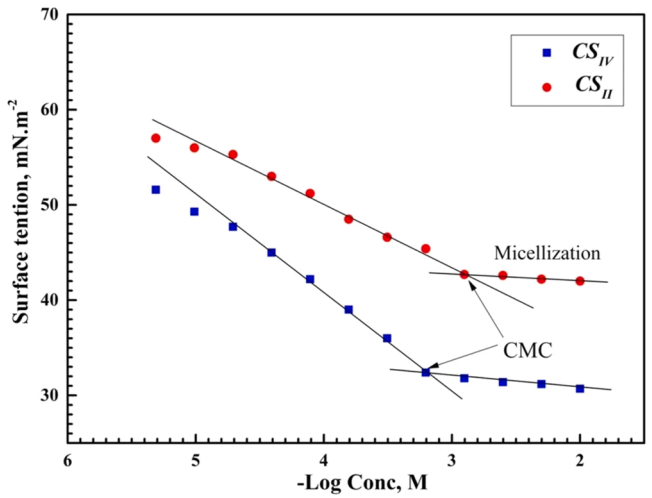

Fig. 1. Surface tension vs. CS_{II} & CS_{IV} cationic surfactant concentrations in 1 M HCl at room temperature.

number of surfactant tails, the tendency toward the micelle formation increases, which means that the surfactant unimers aggregated together at lower concentration (Table Si 1), so affording lowering of the CMC values.

The effectiveness (π_{CMC}) can be defined as the difference between the surface tension value at CMC (γ_{CMC}) and that for the 1 M HCl (γ_o) as follow:

$$\pi_{CMC} = \gamma_o - \gamma_{CMC} \quad (1)$$

Table Si 1 shows the π_{CMC} values for the CS_{II} and CS_{IV}. The results outlined that the CS_{IV} containing 4 hydrophobic tails is the most effective in lowering the surface tension compared to the CS_{II} surfactant. The $\boldsymbol{\pi_{CMC}}$ of CS_{IV}, and CS_{II} surfactant at 25 °C, are 27.6, & 17.3, respectively [14,29]. The high $\boldsymbol{\pi_{CMC}}$ value reflects construction a condensed layer of surfactant unimer at the interface, induced by CS_{IV} surfactant compared to CS_{II} [30], which is expected to be more efficient as corrosion inhibitor material.

The Maximum surface excess ($\boldsymbol{\Gamma_{max}}$) can be defined as the effectiveness of adsorption or accumulation of surfactants molecules at the air/1 M HCl solution interface which is calculated from the slope of the straight line of the post-micellar region (dγ/d InC) using Gibb's adsorption isotherm equation:

$$\Gamma_{max} = \left(-\frac{d\gamma}{dlnC}\right) \Big/ (2.303nRT) \quad (2)$$

where R denotes the gas constant, and T denotes absolute temperature (K). The number of ions dissociation is determined by the number of surfactant molecules adsorbed at the interface in the case of CS_{II} (n = 3) and CS_{IV} (n = 5).

The values of Γ_{max} in Table Si 1 showed that as the number of alkyl hydrophobic chains increased, the values of Γ_{max} increased. When compared with the CS_{IV} cationic surfactant (Γ_{max} =0.0005357) [31,32] counterpart, the CS_{II} cationic surfactant have lower maximum surface excess (Γ_{max} =0.0002152).

The minimum surface area ($\boldsymbol{A_{min}}$) can be defined as the average area of the interface occupied by one molecule in nm^2. Values of A_{min} calculated according to Eq. (3) were listed in Table Si 1.

$$A_{min} = 10^{14} / N_A \Gamma_{max} \quad (3)$$

where N_A represents Avogadro's number [14,17]. The values of A_{min} revealed that increasing the hydrophobic chain number in the cationic surfactant shifted A_{min} to lower values, reaching (A_{min} =619.5 nm) in presence of CS_{IV} cationic surfactant and (A_{min} =319.28 nm) in the presence of CS_{II} cationic surfactant.

The $\boldsymbol{\Gamma_{max}}$ provides information about the CS_{IV} and CS_{II} unimer concentration at the solution interface, while the $\boldsymbol{A_{min}}$ describes their packing density and orientation at interface. Increasing the number of hydrocarbon tail, the $\boldsymbol{\Gamma_{max}}$ increased, while $\boldsymbol{A_{min}}$ decreased (Table Si 1). This reflects that the CS_{IV} surfactant oriented more vertically compared to CS_{II}, therefore the accumulation of the CS_{IV} at the interface is higher compared to CS_{II}.

The change in free energy of micellization (ΔG°_{mic}) and adsorption (ΔG°_{ads}) for the synthesized CS_{II} and CS_{IV} surfactants was calculated and listed in Table Si 1 according to the following equations:

$$\Delta G^{\circ}_{mic} = 2.303RT \log CMC \quad (4)$$

$$\Delta G^{\circ}_{ads} = \Delta G^{\circ}_{mic} - (0.06023 \times \pi_{CMC}/\Gamma_{max}) \quad (5)$$

From the Table Si 1, the negative values of ΔG°_{mic} and ΔG°_{ads} indicate that the micellization and adsorption processes occurred spontaneously. The values of ΔG°_{mic} and ΔG°_{ads} increased with increasing number of hydrophobic chains. So, $CS_{IV} > CS_{II}$ in both micellization and adsorption features. Furthermore, the values of ΔG°_{ads} were more than those of ΔG°_{mic} indicating that the opportunity of the prepared CS_{II} and CS_{IV} to migrate to the air/solution interface is greater than aggregation in micelles after surface saturation (Table 1). Interestingly, the ΔG°_{ads} of the CS_{IV} surfactant inhibitors is more negative (−33.56 kJ mol^{-1}) than the CS_{II} (−32.98 kJ mol^{-1}), indicating its higher adsorption affinity at solution interface, thus higher corrosion inhibition efficiency is expected [14,35].

3.2. Electrochemical measurements (EIS and PDP)

3.2.1. EIS

Nyquist, Bode, and phase angle plots represent the impedance response of C-steel in 1 M HCl with and without various concentrations of CS_{II} and CS_{IV} cationic surfactants represented in Fig. 2 for CS_{IV} and those of CS_{II} in Fig. Si 8. According to Fig. 2 the Nyquist curves were not perfectly circular, and the slope of the linear part of the Bode plot (log Vs log/z/) deviated from − 1. Furthermore, the maximum value of phase angle at the intermediate frequency region deviated from − 90. All of these observations were attributed to frequency dispersion phenomena caused by the roughness and heterogeneity of C-steel surface [20,36]. The diameter of Nyquist curves increases as the concentrations of inhibitors increase, giving consequently a decrease in the corrosion rate due to their adsorption process at C-steel/HCl interface [14,34,35].

It was observed that the shape of Nyquist curves does not change the overall whole inhibitor's concentrations compared to that of the blank. This indicates that the C-steel dissolution reaction mechanism is controlled mainly by charge transfer resistance [17,39,40]. Modulus impedance value /Z/ at low-frequency region and phase angle value at intermediate frequency region in Bode-phase angle plot was increased with CS_{II} and CS_{IV} addition. This indicates to the corrosion rate of C-steel reduced via CS_{II} and CS_{IV} adsorption [37–39].

Table 1 shows the numerical fitting parameters obtained using various equivalent circuits. The EIS spectra of C-steel in pure 1 M HCl and those in treated HCl with CS_{II} and CS_{IV} at molar concentration ranges (1×10^{-6} - 1×10^{-4}) can be fitted with a simple Randles equivalent circuit, whereas the EIS spectra of C-steel in 5×10^{-4} M was better fitted to with a modified equivalent circuit, as shown in Fig. Si 9. This phenomenon may be related to the fact the C-steel reaction is controlled by mass transport at pure and after injection of concentration range (1×10^{-4}: 1×10^{-6}) M of CS_{II} and CS_{IV}, whereas at concentration 5×10^{-4} M of the tested inhibitors the C-steel dissolution mechanism changed due to the formation of stable adsorbed film [28,31,42]. The elements of the equivalent circuit used to fit the obtained experimental data are R_S "solution resistance", *CPE* "constant phase element" defined

Table 1
EIS parameters for C-steel 1 M HCl in absence and presence of different concentrations of CS_{II} and CS_{IV} surfactants at room temperature.

Inh.	Conc, M	R_s, (Ω cm^2)	R_{ct}, (Ω cm^2)	*CPE*		C_{dl}, (F/cm^2) x10^{-6}	R_f (Ω cm^2)	*CPE* (f)		C_{dl} (f) (F/cm^2) x10^{-6}	τ, s	Θ	*IE*%	χ^2 x10^{-3}
				Y^O, sn Ω^{-1} cm^{-2} $\times 10^{-5}$	n			Yf, (s^n Ω^{-1} cm^{-2}) x10^{-6}	n					
Blank	0.00	3.499	28.2	4.26	0.8694	15.515	–	–	–	–	0.00127	–	–	1.777
CS$_{II}$	1×10^{-6}	4.572	170.27	2.01	0.8355	6.573	–	–	–	–	0.002	0.834	83.43	1.520
	5×10^{-6}	3.031	291.19	1.71	0.8464	6.532	–	–	–	–	0.00318	0.903	90.31	1.434
	1×10^{-5}	5.462	388.15	1.601	0.8416	6.154	–	–	–	–	0.00253	0.927	92.73	1.204
	5×10^{-5}	3.589	508.14	1.530	0.8349	5.858	–	–	–	–	0.004	0.944	94.45	1.134
	1×10^{-4}	6.874	649.13	1.209	0.8017	3.645		–	–	–	0.00799	0.956	95.65	0.599
	5×10^{-4}	8.453	753.9	1.119	0.8028	3.463	17.07	4.55	0.786	1.848	0.01006	0.963	96.34	0.043
CS$_{IV}$	1×10^{-6}	3.753	297.29	1.98	0.8215	6.489	–	–	–	–	0.00504	0.905	90.51	1.779
	5×10^{-6}	3.184	397.59	1.67	0.8294	5.989	–	–	–	–	0.00635	0.929	92.90	1.216
	1×10^{-5}	3.333	446.93	1.52	0.8319	5.545	–	–	–	–	0.0065	0.936	93.69	1.394
	5×10^{-5}	3.941	563.54	1.51	0.8192	5.231	–	–	–	–	0.00799	0.949	94.99	1.411
	1×10^{-4}	2.460	682.01	1.198	0.8159	4.049		–	–	–	0.02008	0.958	95.86	0.929
	5×10^{-4}	7.914	806.04	1.101	0.8012	3.409	25.41	2.58	0.816	1.813	0.01267	0.966	96.60	0.149

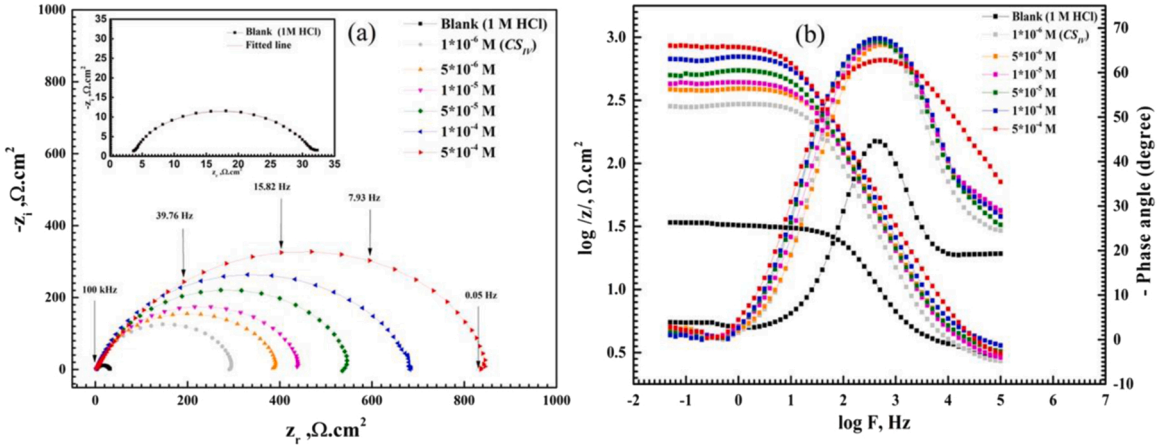

Fig. 2. (a)Nyquist, (b)Bode and phase degree diagrams for C-steel steel in 1 M HCl in absence and presence of different concentration of CS_{IV} cationic surfactants at room temperature.

by Y_o, coefficient n, and R_{ct} "polarization resistance ($R_{ct1} + R_f$) to give more accurate fitting parameters as the C_{dl} affected by surface imperfection" [21,26,41]. The inhibited solution has lower (n) values than the free acid solution ($0 > n > 1$), indicating that presence of the inhibitor increases surface heterogeneity due to accumulation or /and adsorption at the C-steel/1 M HCl solution interfaces [41,42].

Table 1 shows that R_S values increase due to cationic species of CS_{II} and CS_{IV} adsorption on the C-steel [43,44]. The surface coverage (θ) and the inhibition efficiency (*IE*%) listed in Table 1 were calculated based on R_{ct} values according to equations:

$$\theta = (R_{ct.inh} - R_{ct.blank})/R_{ct.inh}) \quad (6)$$

$$IE\% = \theta \times 100 \quad (7)$$

C_{dl} and relaxation time (τ) [46] values listed in Table 1 were calculated according to equations:

$$C_{dl} = (Y_o R_{ct}^{1-n})^{1/n} \quad (8)$$

$$\tau = C_{dl} \times R_{ct} \quad (9)$$

The data in Table 1 show that R_{ct} value of C-steel increases with the addition of cationic surfactant molecules, even at low concentration (1×10^{-6} M) to 297.29 Ω.cm^2 and 170.27 Ω.cm^2 for CS_{IV} and CS_{II} cationic surfactants, respectively compared to the blank 28.2 Ω.cm^2. Then, as concentrations increased, their values increased till touch 770.79 Ω.cm^2 and 831.45 Ω.cm^2 at 5×10^{-4} M of CS_{II} and CS_{IV} cationic surfactants, respectively. This behavior can be explained by the adsorption of CS_{II} and CS_{IV} on the C-steel surface forming a protective film layer. This finally reduces the contact between the C-steel surface and corrosive HCl solution and thus decreasing the C-steel corrosion rate [36,48,49]. C_{dl} values, on the other hand, decreased as concentration increased. This behavior is explained by the formation of a protective film due to the inhibitor's adsorption via active centers such as: hetero atoms in amide groups (O═C-NH), *pz* orbitals of pyridine rings, and charged quaternary amines. According to Helmholtz model in Eq. (10), C_{dl} values due to the gradually replacement of adsorbed water molecules/Cl^- ions by the molecules of the tested compounds. This leads to decrease the subjected surface area of the electrode (A) and increase the thickness of adsorbed film (T) [49–51].

$$C_{dl} = \left(\frac{\varepsilon^{\circ}\varepsilon}{T}\right)A \quad (10)$$

where $\varepsilon\circ$ is the permittivity of air and ε is the local dielectric constant [14,45]. Table 1 shows that in presence of 5×10^{-4} M of CS_{II} and CS_{IV} cationic surfactant, the relaxation time (τ) value increased to 0.01006 s and 0.012667 s, respectively compared to the free acid solution 0.00127 s. This indicated that the adsorption process takes much longer time, indicating that slow adsorption occurs. This confirmed the application of modified equivalent circuit to fit the data correctly also indicated the formation of stable barrier film shielded the C-steel surface

away from the deterioration action of HCl [16,52]. It is worthy noted that, higher number of hydrophobic chains of CS_{IV} enhances its adsorption power at the C-steel interface than that of CS_{II}.

3.2.2. PDP

Fig. 3 depicts representative potentiodynamic polarization curves of C-steel in 1 M HCl solution with and without various concentrations of synthesized CS_{II} and CS_{IV} surfactants. Table 2 shows the electrochemical kinetic parameters extracted based on the extrapolation method of Tafel lines, such as corrosion potential (E_{corr}), cathodic (β_c), and anodic (β_a) Tafel slopes, and corrosion current density (I_{corr}). Surface coverage (θ) and the inhibition efficiency (IE %) were calculated by equations:

$$\theta = (I_{corr.blank} - I_{corr.inh})/I_{corr.blank} \quad (11)$$

$$IE\% = \theta \times 100 \quad (12)$$

where, $I_{corr.blank}$ and $I_{corr.inh}$ are the corrosion current densities for C-steel in the absence and presence of the CS_{II} and CS_{IV} surfactants [53,54].

The I_{corr} in presence of cationic surfactants decrease with increasing their concentrations until reach 32.9 μA.cm^{-2}and 25.9 μA.cm^{-2} at high concentration (5×10^{-4} M) of CS_{II} and CS_{IV} cationic surfactants, respectively, indicating that the synthesized surfactants retard the iron dissolution rate due to their adsorption affinity [12,55]. The presence of CS_{II} and CS_{IV} causes a slight change in (β_c) and (β_a) values. Also, slight variations were noticed in E_{corr} values (<85 mV), suggesting that these compounds acted as mixed-type inhibitors by blocking the cathodic and anodic sites forming a protective film on C-steel surface through the active centers and +ve charges contained in its structures without changing the corrosion mechanism [18,56]. The i-v response curves of C-steel in absence and presence of the tested CS_{II} and CS_{IV} surfactants had nearly the same shape. This confirmed the C-steel reaction mechanism remains unchanged [16,57]. According to Fig. 3, the addition of different concentrations of the prepared CS_{II} and CS_{IV} cationic surfactants stifled the rate of hydrogen evolution (cathodic process) and dissolution reactions (anodic process) of C-steel via increasing the overpotential of C-steel corrosion reactions [58–60]. The parallel in cathodic Tafel lines indicates that hydrogen evolution was activated-controlled. The HER mechanism of C-steel unaffected by the addition of the inhibitors and its rate was slowed by adsorbed inhibitors molecules [14,56].

According to the anodic polarization response of the C-steel shown in Fig. 3, the anodic inhibition effect of the CS_{II} and CS_{IV} depends on the potential applied. These compounds have an inhibition effect only at potentials than − 0.2 V, and no further effect has been detected above this potential. This potential is known as the desorption potential [16]. At higher anodic potential more than the desorption potential (−0.2 v Vs OCP) the desorption rate of CS_{II} and CS_{IV} was greater than their adsorption one [61,62]. The relation between values of I_{corr} and concentrations of the tested cationic surfactants was represented as straight lines as in Fig. Si 10 (a). following the equation:

$$I_{corr} = x - y\log C \quad (13)$$

where x and y are constants. This indicates that, the rate of C-steel corrosion decreases as a result of the adsorption of cationic surfactant molecules on C-steel surface [16,63]. According to the stern-Geary Eq. (4), the values of polarization resistance (R_p) of the C-steel are function of I_{corr} according to the following equation:

$$R_p = \frac{B}{I_{Corr}} \quad (14)$$

where, B is constant [$= (\beta_a\beta_c)/2.303(\beta_a + \beta_c)$] [47-49]. The adsorption of cationic molecules increases the polarization resistance of iron obstructing the active centers and thereby reducing the rate of corrosion. Linear relationship between $1/R_p$ as a measure of corrosion rate and log concentration is represented as in Fig. Si 10 (b) according to the equation:

$$R_p^{-1} = a_1 - b_1\log C \quad (15)$$

where a_1 and b_1 are constants [16]. The R_p values increase as inhibitor concentrations increase, increasing the number of adsorbed molecules. This suggests that these compounds are effective inhibitors [16,50]. Also, the R_p values are a function of the number of hydrophobic chains in CS_{II} and CS_{IV}. As the concentration increased more molecules of CS_{II} and CS_{IV} accumulated over the C-steel and retrained the corrosion process to a high extent. At concentration 5×10^{-4} M of the tested CS_{II} and CS_{IV} compounds, the polarization resistance R_p was 739.39 Ω.cm^2 and 865.35 Ω.cm^2 respectively, this shows that CS_{IV} of higher molecular weight (more number of alkyl chains) covers the higher surface area of C-steel subjected to the aggressive solution so it showed higher inhibition efficiency than CS_{II} similar to PDP output data [64]. So, the EMs are in a good agreement with each other.

It is worth noting that R_p values obtained from the PDP technique were close to the R_{ct} values of the EIS and this boosted the confidence in the experimental data. According to the surface parameters of the CS_{II} and CS_{IV} surfactant inhibitors discussed previously expected the performance of both materials as corrosion inhibitors. The effectiveness

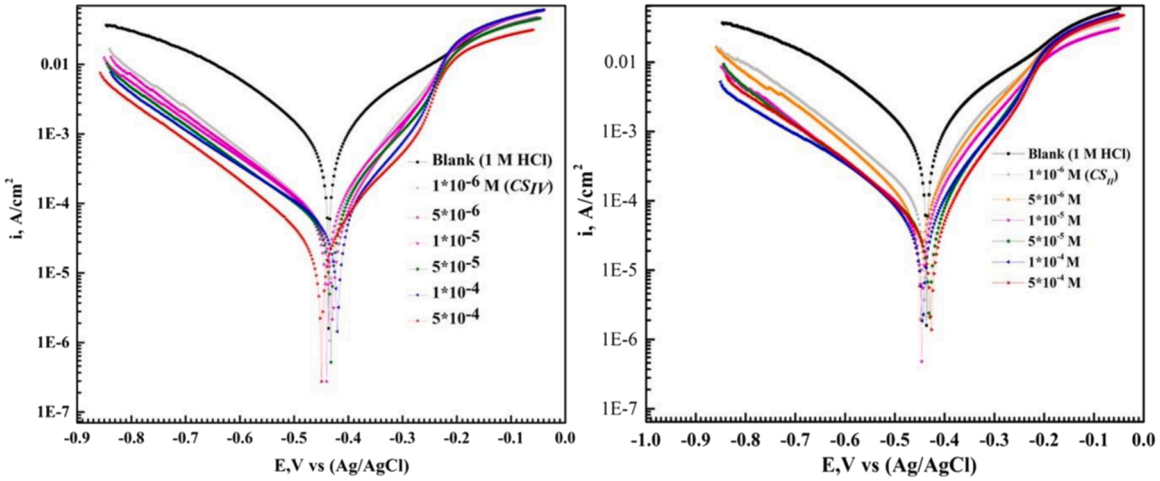

Fig. 3. Potentiodynamic polarization curves for C-steel steel in 1 M HCl in absence and presence of different concentration of CS_{II} and CS_{IV} cationic surfactants at room temperature.

Table 2
Tafel parameters for C-steel in absence and presence of different concentrations of CS_{II} and CS_{IV} surfactants at room temperature.

Inh.	Conc, M	E_{corr}, (V) Vs. Ag/AgCl	I_{corr} (μA/cm^2)	β_a (mV/dec)	β_c (mV/dec)	*r* (mm/year)	R_p (Ω.cm^2)	θ	*IE*%
Blank	0.00	-0.4492	867 ± 15	115.65	153.46	10.071	33.03	–	–
CS$_{II}$	1×10^{-6}	-0.4509	106 ± 2	81.54	141.56	1.2299	211.94	0.8778	87.78
	5×10^{-6}	-0.4486	70.4 ± 1.1	80.45	140.88	0.81775	315.84	0.9188	91.88
	1×10^{-5}	-0.4626	64.2 ± 1	90.5	145.56	0.7455	377.43	0.9259	92.59
	5×10^{-5}	-0.4419	53.3 ± 0.4	100.95	152.3	0.56167	494.58	0.9384	93.84
	1×10^{-4}	-0.4419	41.2 ± 0.2	98.75	154.5	0.4789	634.93	0.9524	95.24
	5×10^{-4}	-0.4243	32.9 ± 0.1	86.649	158.5	0.38249	739.39	0.9620	96.20
CS$_{IV}$	1×10^{-6}	-0.4369	76.5	89.54	149.8	0.88857	318.10	0.9117	91.17
	5×10^{-6}	-0.4467	65.1	90.54	152.24	0.75598	378.69	0.9249	92.49
	1×10^{-5}	-0.4286	52.5	92.41	153.24	0.61058	476.78	0.9393	93.93
	5×10^{-5}	-0.4407	47.8	101.54	149.87	0.55505	549.85	0.9448	94.48
	1×10^{-4}	-0.4249	38.1	97.65	143.54	0.4892	662.32	0.9560	95.60
	5×10^{-4}	-0.4524	25.9	81.54	140.65	0.30595	865.35	0.9701	97.01

(π_{CMC}) depicted in Table Si 1 outlined that the CS_{IV} containing 4 hydrophobic tails is the most effective in lowering the surface tension compared to the CS_{II} surfactant. The high $\boldsymbol{\pi_{CMC}}$ value reflects construction a condensed layer of surfactant unimers at the interface, induced by CS_{IV} surfactant compared to CS_{II} [65], which is expected to have higher inhibition efficiency compared to CS_{II} inhibitor which is confirmed from the electrochemical measurements depicted in Tables 1 and 2, where CS_{IV} surfactant showed higher corrosion inhibition efficiency than CS_{II}. Additionally, the ΔG°_{ads} of the CS_{IV} surfactant inhibitors is more negative than that of the CS_{II}, indicating its higher adsorption affinity at solution interface, thus higher corrosion inhibition efficiency is expected [14,35], which is matched with the inhibition efficiency depicted in Tables 1 and 2, where CS_{IV} surfactant showed higher corrosion inhibition efficiency than CS_{II}.

The as-obtained inhibition efficiencies for the CS_{II} and CS_{IV} were much higher than many previously reported inhibitors in the same electrolyte (1 M HCl) see Table 3 [11,26,66,67].

3.3. Adsorption isotherm

The inhibition performance of the synthesized surfactants can be explained by their competitive adsorption on the metal surface, based on the quasi-substitution process between surfactant molecules and the already adsorbed water molecules at metal/solution interface according to the equation:

$$CS_{sol} + zH_2O_{ads} \leftrightarrow CS_{ads} + zH_2O_{sol} \tag{16}$$

Values of θ of CS_{II} and CS_{IV} cationic surfactants obtained from EIS and PDP data are used to explain the nature of the adsorption process that occurred at C-steel/HCl interface. In this study, several adsorption isotherm models used such as Frumkin, Temkin, Flory, Alawady, Freundlich are shown in Figs. Si 11 and 12, while the Langmuir isotherm is shown in Fig. 4 [14,68]. The output parameters of the applied isotherms are recorded in Table Si 3, while those of Langmuir isotherm are listed in Table 4. Based on the values of R^2, Langmuir isotherm is considered as the best model to describe the adsorption mechanism (Table 4).

$$C/\theta = \left(\frac{1}{K_{ads}}\right) + C \tag{17}$$

where, C and K_{ads} are the inhibitor concentration(M) and the equilibrium constant of the adsorption process, respectively [69]. The intercept of Fig. 4 gives K_{ads} values. Higher K_{ads} values explained the strength of the inhibitor-Fe bond formed via donor-acceptor interaction between active centers of CS_{II} and CS_{IV} structures and the uncompleted 3d-orbital of iron forming a strong chemical bond [70]. The fundamental characteristic of Langmuir isotherm R_L (dimensionless separation factor) was calculated using the equation:

$$R_L = 1/(1 + K_{ads}C) \tag{18}$$

Values of R_L listed in Table Si 4 were less than unit (R_L<1) which mean high and favorable adsorption affinity of CS_{II} and CS_{IV} over C-steel [18]. The change in the standard free energy of adsorption (ΔG^*_{ads}) calculated from the following equation were listed in Table 4:

$$\Delta G^*_{ads} = -RT\ln(55.5K_{ads}) \tag{19}$$

where the value 55.5 is molar concentration water [29]. The calculated values of ΔG^*_{ads},− 44.90 and − 45.19 kJ mol^{-1} for CS_{II} and CS_{IV} respectively, indicate the chemical adsorption formed via hetero atoms (N & O) and pyridine ring. And also, their negative sign indicate the adsorption process occurs spontaneously [29,70].

Table 3
comparison between corrosion inhibition of CSII and CSIV cationic surfactants and other investigated cationic surfactants for C-steel in 1 M HCl.

Compound	Concentration	*IE*%		Ref.
		PDP	EIS	
12-E2–12	1×10^{-2}	66.36	68.3	[11]
14-E2–14	1×10^{-2}	77.77	71	
I(4 N)	1×10^{-3}	92	91.99	[26]
II(4 N)	1×10^{-3}	95	94.93	
IV(4 N)	1×10^{-3}	96	95.84	
IL2	5×10^{-3}	89.18	90.55	[66]
IL	5×10^{-3}	90.82	92.41	
IL6	5×10^{-3}	93	94.09	
DHNMMB	2.5×10^{-3}	94.16	93.93	[67]
DHNBMBDMB	2.5×10^{-3}	95.06	95.4	
CS$_{II}$	5×10^{-4}	96.202	96.3	Present study
CS$_{IV}$	5×10^{-4}	97.01	96.6	

3.4. Activation thermodynamic parameters

PDP curves of C-steel in absence and presence 5×10^{-4} M of CS_{II} and CS_{IV} are shown in Fig. Si 13 and their relevant parameters are listed in Table Si 5. It is noticed that the dissolution rate of the C-steel and the corrosion current density increase as temperature increase. According to Table Si 5, rising temperature has no discernible effect on the CS_{II} and CS_{IV} inhibition efficiencies, implying that these compounds have a chemical adsorption behavior [35].

Thermodynamic activation parameters E_a "activation energy", ΔH* "activation enthalpy" and ΔS* " activation entropy" using Arrhenius and Transition state equations:

$$\ln r = \ln A - \left(\frac{E_a}{RT}\right) \tag{20}$$

$$\ln(r/T) = \left[\ln\left(\frac{R}{N_A h}\right) + \left(\frac{\Delta S^*}{R}\right)\right] - \left(\Delta H^* \Big/ RT\right) \tag{21}$$

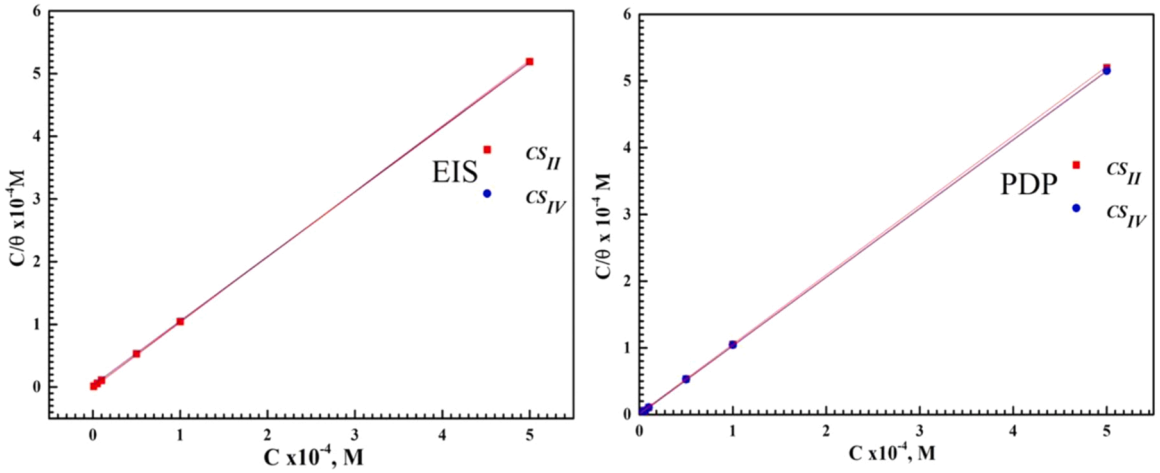

Fig. 4. Langmuir adsorption isotherm of CS_{II} and CS_{IV} at C-steel/HCl. interface using EIS and PDP techniques at room temperature.

Table 4
Langmuir isotherm model parameters of C-steel in absence and presence of CS_{II} and CS_{IV} surfactants.

	PDP				EIS			
Inh.	*Slope*	R^2	$LogK_{ads}$, ($L.mol^{-1}$)	ΔG°_{ads} ($kJmol^{-1}$)	*slope*	R^2	$LogK_{ads}$, ($L.mol^{-1}$)	ΔG°_{ads} ($kJmol^{-1}$)
CS_{II}	1.0386	0.9999	6.19874	-44.553	1.03709	1	6.262	-44.908
CS_{IV}	1.0299	0.9999	6.16138	-44.343	1.03334	1	6.31286	-45.193

where, *r*, A represented corrosion rate of reaction and Arrhenius constant respectively and, R is the gas constant. *h* and N_A are Plank constant and Avogadro's number [71]. Values of E_a estimated from the slope of Fig. 5 are listed in Table 5. In presence of CS_{II} and CS_{IV}, the E_a values are seemed to be unchanged as seen in Table 5. This confirms that the adsorption of CS_{II} and CS_{IV} on the C-steel surface is almost of the chemical adsorption type. The E_a of CS_{IV} is lower than that of CS_{II} confirming that CS_{IV} adsorbed chemically on C-steel surface [72].

Fig. 5 showed plotting of Ln(*r*/T) vs. (1/T) as a straight line with slope (=-ΔH*/R) and an intercept (=[Ln(R/N_A*h*)+ (ΔS*/R)) [73-75]. From Table 6, the +ve sign of ΔH* shows the endothermic nature of the corrosion process C-steel. This indicated the difficulty of the C-steel corrosion process in presence of CS_{II} and CS_{IV} compared to free acid solution [62,63]. The -ve sign of ΔS* indicates that the rate-determining step was the activation of the complex rather than the dissociation. This meant that there was more order, which led to an increase in inhibition efficiency (from reactant to activated complex)[62,63].

3.5. Film stability under harsh conditions

Aside from a strict requirement for highly efficient corrosion inhibitor activity, the film durability under corrosion operation is also critical. To investigate the durability of adsorbed film of CS_{II} and CS_{IV} layer formed over a C-steel surface at 5×10^{-4} M the inhibition efficiency values measured at different temperatures and immersion times using the EIS test method.

3.5.1. Temperature effect

Non-tangible change in inhibition efficiency over the tested temperature range (20 °C:60 °C). Data recorded in Table Si 6 showed the change in the inhibition efficiency percentage has not exceeded one percent. This indicated the formation of a chemical bond between the 3d-orbital of iron and the adsorption centers of CS_{II} and CS_{IV} compounds [22,31]. It was noticed that the solution resistance (R_S) decreased with elevation temperature. This revealed that increasing electrolyte conductivity was caused by the desorption of some cationic CS_{II} and CS_{IV}

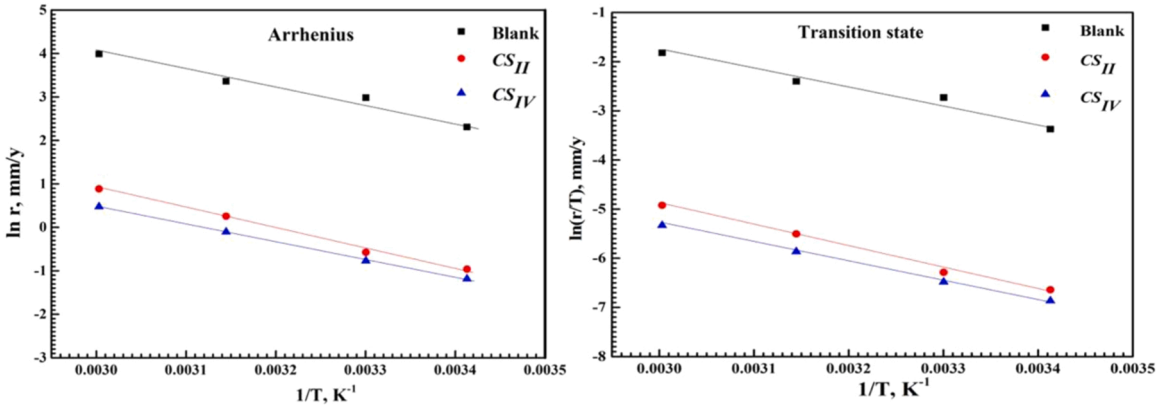

Fig. 5. Arrhenius and transition state relation against 1/T, for C-steel in 1 M HCl in absence and presence of 5×10^{-4} M of CS_{II} and CS_{IV} cationic surfactants.

Table 5
Activation thermodynamic parameters of C-steel in absence and presence of CS_{II} and CS_{IV} surfactants.

Inh.	Arrhenius				Transition state			
	Slope	*Intercept*	R^2	E_a (kJ mol^{-1})	*Slope*	*Intercept*	ΔH* (kJ mol^{-1})	-ΔS* (J mol^{-1})
Blank	-3873.99	15.617	0.9757	32.208	-3561.81	8.872	29.612	123.752
CS_{II}	-4617.25	14.747	0.995	38.387	-4305.06	8.002	35.792	130.987
CS_{IV}	-4080.94	12.726	0.9994	33.928	-3768.76	5.981	31.333	147.788

Table 6
Quantum chemical parameters of the investigated CS_{II} and CS_{IV} compounds.

Quantum parameters	CSII	CSIV
EH (eV)	-9.165	-8.672
EL (eV)	-1.369	-2.348
ΔE(eV)	7.796	6.324
X (eV.mol-1)	5.267	5.51
η (eV. mol-1)	3.898	3.162
$E_{b\to d}$(eV. mol-1)	-0.9745	-0.7905
ΔN	0.222293	0.23561

species.

3.5.2. Effect of immersion time

The inhibition efficiency values in presence of CS_{II} and CS_{IV} were measured over a long exposure time presented in Table Si 7. With increasing immersion time, the *IE*% values increase slightly. This is because the stability of the protective layer formed as a result of CS_{II} and CS_{IV} molecules' adsorption and/or accumulation on the C-steel surface which leads to slow the aggressive action of HCl [33,76]. However, from Fig. Si 14 it is noticed that the values of R_{ct} in HCl solution decreased with time, indicating that dissolution of carbon steel (corrosion process) increased with the immersion time. In the presence of CS_{II} and CS_{IV}, all R_{ct} values were significantly high, indicating that an adsorbed inhibitor film protects the C-steel surface from the aggressive action of acidic HCl solutions. The decrease in R_{ct} of inhibited solutions with different exposure times could be explained by the desorption of a small amount of adsorbed CS_{II} and CS_{IV} molecules from the surface, as well as some defects on the film layer caused by the acidic HCl's aggressive action [23,35]. The inhibition performance of CS_{II} and CS_{IV} under highly aggressive conditions caused by temperature and longer exposure time endows CS_{II} and CS_{IV} have the tendency for use as acidic corrosion inhibitors in industrial process.

3.6. Theoretical quantum chemical study

The relation between *IE*% and the molecular structure of CS_{II} and CS_{IV} compounds has been discussed theoretically using DFT. The optimized structure, highest occupied molecular orbital (HOMO), lowest unoccupied molecular orbital (LUMO), and electron density (ED) of CS_{II} and CS_{IV}, which determine the adsorption active centers in the molecular structure, are shown in Fig. 6. The optimized structure represents the most stable structure of CS_{II} and CS_{IV}. The ability of CS_{II} and CS_{IV} to donate and receive electrons to or/and from C-steel atomic d-orbitals represented by the energies of HOMO and LUMO [3,77]. It can be noticed from Fig. 6 that the electron clouds are only distributed, respectively over the quaternary nitrogen atoms and pyridine moieties for HOMO and LUMO of the tested compounds. This means that these areas participated effectively in the charge-sharing process (electron donation/acceptance). These regions represent the donor-acceptor interaction centers responsible for interaction with carbon steel. Furthermore, the distributed electron density of CS_{II} and CS_{IV} over their entire molecular structures endows them with the ability to form dense adsorbed layers on the C-steel surface. The remaining molecular components (alkyl chains) of the molecular structures only served to increase the affinity CS_{II} and CS_{IV} to be compacted or adsorbed on the C-steel surface; they did not form bonds with the surface. The presence of hydrophobic chains in the solution increases the adsorption affinity of CS_{II} and CS_{IV} [64].

The energies of HOMO (E_H) and LUMO (E_L) are used to deduce the relative quantum indices according to the following equations:

$$\Delta E_{gap} = E_L - E_H \tag{22}$$

$$\eta = \frac{\Delta E_{gap}}{2} \tag{23}$$

$$E_{b\to d} = \frac{-\eta}{4} \tag{24}$$

$$\chi = \frac{-(E_H + E_L)}{2} \tag{25}$$

$$\Delta N = \frac{(\varphi_{Fe} - \chi_{compd.})}{[2((\eta_{Fe} + \eta_{compd.})]} \tag{26}$$

where, ΔE_{gap}, η, χ, ΔN, $E_{b\to d}$ and φ are energy gap, global hardness, electronegativity, the fraction of transferred electron, the energy of back donation, and work function of Fe (1 1 0) plan is 4.82 eV [16,77]. The affinity of CS_{II} and CS_{IV} compounds to donate electrons to the uncompleted 3-d iron orbitals and accept electrons from the full-field 3-d iron orbitals is a function of the energy of HOMO and LUMO, respectively. The data of Table 6 showed that the CS_{II} and CS_{IV} compounds have a higher affinity to donate and accept electrons to /or from 3-d iron orbital. This indicated the corrosion inactivator potential of the C-steel. Furthermore, CS_{IV} has a higher chance to be adsorbed over C-steel as it had higher E_H and lower E_L compared with CS_{II} [64]. Furthermore, the energy gab ΔE_{gap} parameter indicates the ease of the charge sharing process. The lower the ΔE_{gap} value, the greater the chance of charge-sharing and the greater the potential for the corrosion inhibition [78]. As a result, CS_{IV} has a greater adsorption affinity than CS_{II} due to its lower value of ΔE_{gap}. In addition, the positive values of the fraction of the electron transfer (ΔN) parameter means that electrons are transferred from HOMO of CS_{II} and CS_{IV} compounds to C-steel. ΔN reported values show that the inhibition order of the tested compounds was CS_{II} >CS_{IV}. Finally, the back-donation process, which involves the electron acceptance affinity of CS_{II} and CS_{IV} compounds from the C-steel surface, improves their adsorption probability [79]. The calculated DFT parameters matched with the experimental data (EIS and PDP). The DFT calculations should be supplemented with molecular simulation to provide a complete picture of the inhibitory mechanism and to gain a better understanding of the adsorption process of the understudied cationic surfactant compounds (CS_{II} and CS_{IV}). To simulate the corrosion reaction conditions, MC simulation was performed in vacuum and solvent phases. Fig. 7 depicts the most stable adsorption configuration of CS_{II} and CS_{IV} compounds with low energy over the Fe (110) plain in gas and simulated acidic solution phases. The side and top views of CS_{II} and CS_{IV} configurations give valuable information that supports the DFT output data and can be discussed point by point briefly as follow:

- Side views in gas and solvent phases showed the parallel orientation of CS_{II} and CS_{IV} to Fe (110) plan

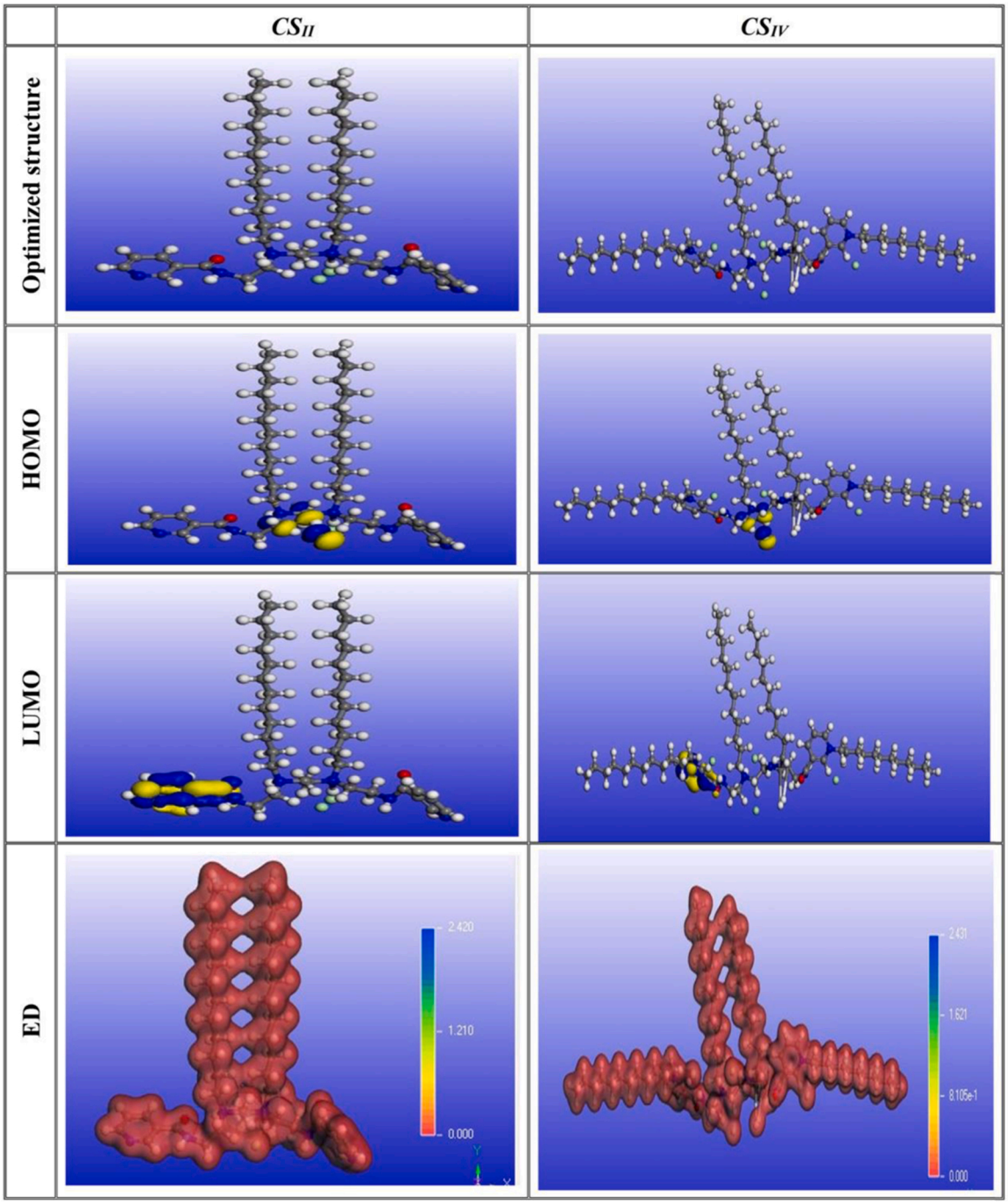

Fig. 6. Optimized structures, HOMO, LUMO, and electron density distribution of CS_{II} and CS_{IV} cationic surfactants in gas and phase.

- Top views also, showed the CS_{II} and CS_{IV} compounds occupy and cover a large area of Fe (110) surface.

Orientation of CS_{II} and CS_{IV} on Fe (110) plan confirmed the suggested electron-rich moieties (nitrogen and pyridine rings) subjected directly to C-steel. This improved the inhibition performance of CS_{II} and CS_{IV} compounds by facilitating electron transfer during the charge sharing process [78]. In addition, the hydrocarbon chain length was oriented parallel to Fe (110) to increase the coverage surface area and improve the inhibition affinity of CS_{II} and CS_{IV} compounds [80,81]. Chain length in CS_{IV} subjected also, toward the solvent side made the adsorption film formed over C-steel more compacted and denser. Table 7 shows the output adsorption energy parameters (E_{ads}) for CS_{II} and CS_{IV}, which confirmed their adsorption affinity. The adsorption of CS_{II} and CS_{IV} on C-steel is more stable and powerful the larger the negative value of E_{ads} [79,82].

As was already established, CS_{IV} has stronger adsorption competition with molecules of H_2O, H_3O^+, and Cl^- ions. This conclusion is in line with the EIS data that was previously addressed and shown the propensity of CS_{IV} compounds to take the place of these hostile ions in the C-steel interface.

3.7. Surface analysis (SEM and EDX) and inhibition mechanism

SEM and EDX are used in addition to electrochemical measurements to investigate the corrosive effect of 1 M HCl and the inhibitory effect of

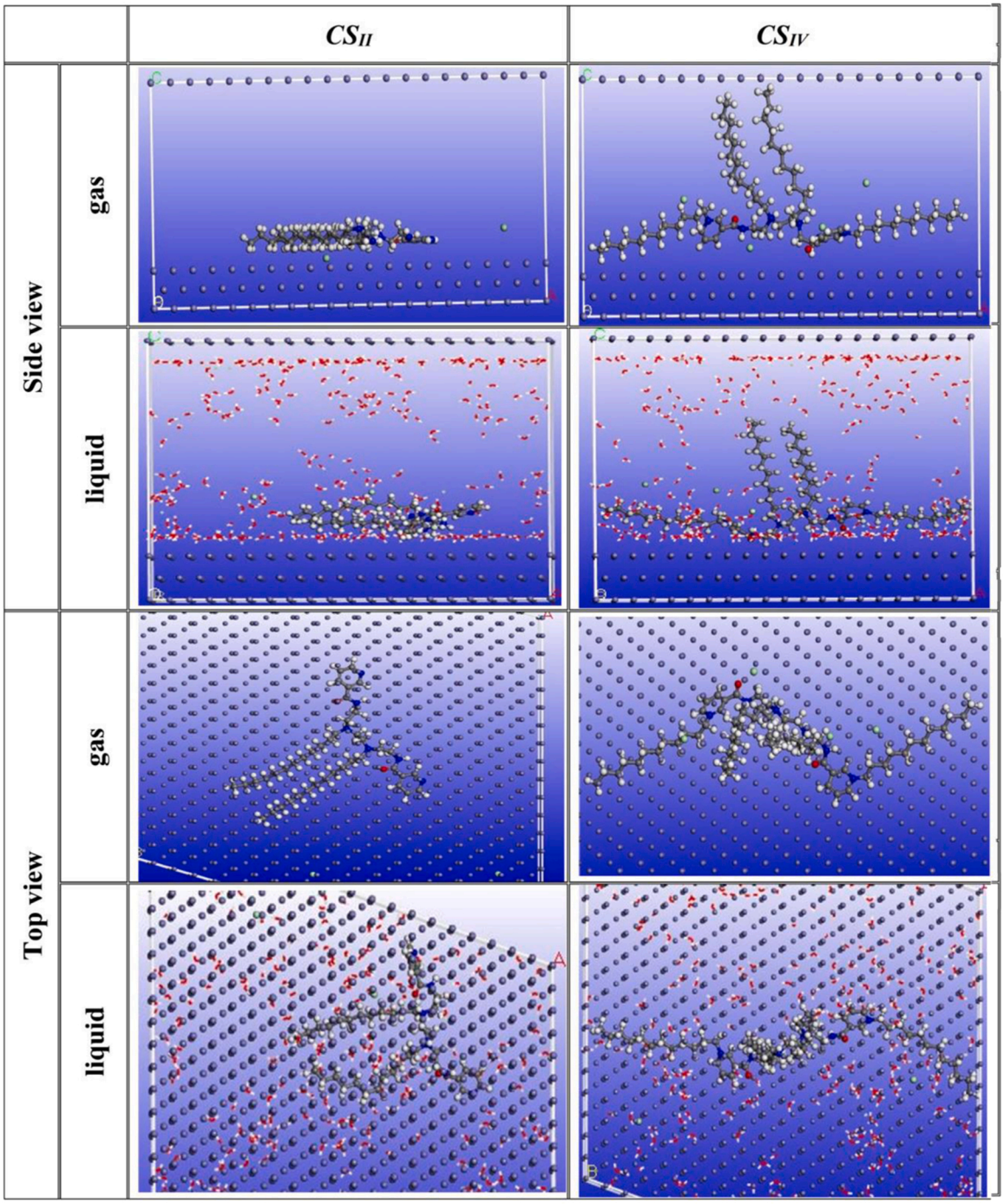

Fig. 7. Side and top views of the adsorption mode of CS_{II} and CS_{IV} cationic surfactants in gas and liquid phases on Fe (1 1 0).

Table 7
The outputs energies calculated using MCs for CS_{II} and CS_{IV} in gas and simulated liquid phases on Fe (1 1 0).

Inh.		E_T (kJ/mol)	E_{ads} (kJ/mol)	$E_{rig.}$ (kJ/mol)	$E_{def.}$ (kJ/mol)	(dE_{ads} /dNi) (kJ/mol)			
						CS-surfactant	H_2O	H_3O^+	Cl^-
Gas	CS_{II}	-517.1094	-1222.46	-395.39	-827.07				
	CS_{IV}	-628.648	-140489.60	-462.85	-140026.70				
liquid	CS_{II}	-4096.18	-10740.35	-4093.72	-6646.63	-1141.10	-19.7427	-164.732	-131.293
	CS_{IV}	-4349.92	-150140.00	-4356.95	-145783.10	-140692.80	-19.973	-171.860	-120.321

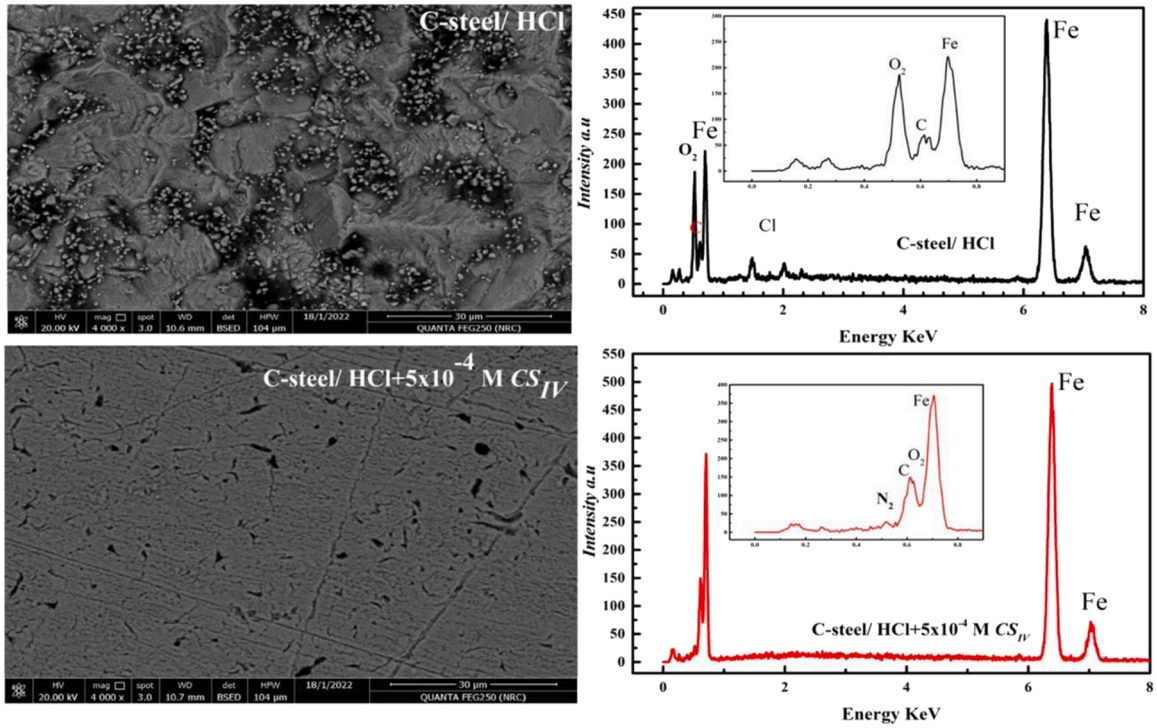

Fig. 8. SEM and EDX for C-steel after 6 h immersion in pure1 M HCl and 5×10^{-4} M of CS_{IV} compound.

CS_{IV} at optimum concentrations. Fig. 8 shows surface images for C-steel with and without inhibitors immersed in 1 M HCl for 6 h. In the absence of CS_{IV} compound, SEM images reveal damage and dissolution of the C-steel surface with many corrosion products (Fe-chloride and oxides) [50, 83]. This damage effect seemed under control in the presence of 5×10^{-4} M of highly effective compound (CS_{IV}) and the surface of C-steel became more smoother compared with that subjected to the free acid solution. This confirms the adsorption of CS_{IV} molecules on the C-steel surface and formation of a protective surface coverage film as a barrier between C-steel and corrosive HCl. This observation was consistent with previously published work [16].

The elemental chemical composition of C-steel after 6 h immersion in 1 M HCl appeared in Fig. 8. The chemical composition of the corrosion product formed over the C-steel surface was iron oxides and chlorides as the weight percentage of Cl^- and oxides was 0.19% and 10.679%, respectively. After adding the 5×10^{-4} M of highly effective compound (CS_{IV}) it is noticed that, the weight percentage of the oxides decreased to 1.63% and the chloride is nearly disappeared. In addition to that, the wt% of carbon enhanced to 8.53% and the appearance of N-peak with wt% 1.38%. This confirms the formation of adsorption layer from the smooth iron oxides and CS_{IV} compound with high carbon backbone and nitrogen atom over C-steel surface. It is noted that the Fe-peak intensity improved after the addition of CS_{IV}. This confirms that the C-steel surface becomes free of corrosion products and more susceptible to the EDX beam [24,84]. These observations were cross-checked against previously published papers [84,85]. Fig. 9 showed the simulated adsorption mechanism of CS_{IV} cationic surfactant over C-steel.

4. Conclusion

In this study, the chemical structures of the two synthesised Gemini surfactant compounds, CS_{II} and CS_{IV}, were confirmed by various spectroscopic methods. The experimental and theoretical findings show that the studied compounds (CS_{II} and CS_{IV}) exhibit good inhibition

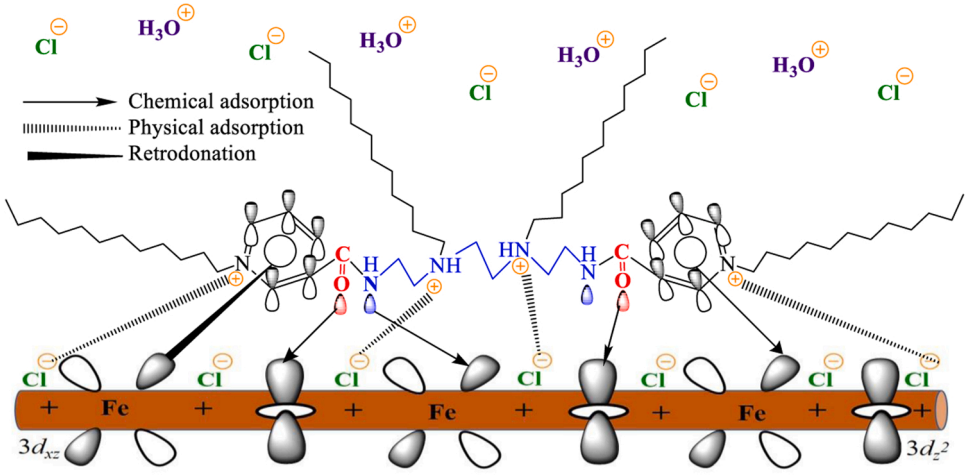

Fig. 9. Adsorption mechanism of CS_{IV} cationic surfactant over C-steel.

performance for C-steel in 1.0 M HCl solution. The polarization studies suggest that CS_{II} and CS_{IV} behave as mixed-type corrosion inhibitors according to Tafel data. The electrochemical impedance results show that the R_{ct} value of CS_{II} and CS_{IV} increased from 28.2 Ω.cm^2 to 770.97 Ω.cm^2 and 831.45 Ω.cm^2, respectively. This suggests that the C-steel corrosion is essentially under charge transfer control, where the formation of adsorbed protective layer, inhibits the steel corrosion. Also, CS_{II} and CS_{IV} were found to adsorb chemically at C-steel according to Langmuir adsorption isotherm. The SEM coupled with the EDX confirm the formation of protective layer over C-steel. DFT calculations and Monte Carlo (MC) simulations give a better overview of the reactivity of both compounds towards C-steel and show good correlation with the experimental results.

CRediT authorship contribution statement

A. Elaraby: Investigation, Methodology, Data curation, Writing – original draft. **M. Abd-El-Raouf:** Supervision, Validation, Writing – review & editing, Investigation, Methodology. **M.A. Migahed:** Supervision, Validation, Writing – review & editing, Investigation, Methodology. **A.S. El-Tabei:** Validation, Writing - review & editing. **A. M. Abdullah:** Supervision, Validation, Writing – review & editing, Data curation. **N. Al-Qahtani:** Supervision, Validation, Writing – review & editing, Investigation, Methodology, Data curation. **Sami M. Alharbi:** Validation, Writing – review & editing. **Samy M. Shaban:** Supervision, Validation, Writing – review & editing, Investigation, Methodology, Data curation. **Dong-Hwan Kim:** Supervision, Validation, Writing – review & editing. **Amr Elgendy:** Validation, Writing – review & editing. **N.M. El Basiony:** Supervision, Investigation, Methodology, Data curation, Writing – review & editing.

Declaration of Competing Interest

The authors declare that they have no known competing financial interests or personal relationships that could have appeared to influence the work reported in this paper.

Data availability

Data will be made available on request.

Acknowledgments

This work was supported by the National Research Foundation of Korea (NRF) grant funded by the Korea government (MSIT and Ministry of Education) (2022H1D3A2A02060789, 2021H1D3A2A02096291 and 2019R1A2C2085177). The authors are also grateful to the Egyptian Petroleum Research Institute (EPRI) and the Center for Advanced Materials (CAM) for their support.

Appendix A. Supplementary material

Supplementary data associated with this article can be found in the online version at doi:10.1016/j.colsurfa.2022.130687.

References

[1] S. Javadian, B. Darbasizadeh, A. Yousefi, F. Ektefa, N. Dalir, J. Kakemam, Dye-surfactant aggregates as corrosion inhibitor for mild steel in NaCl medium: experimental and theoretical studies, J. Taiwan Inst. Chem. Eng. 71 (2017) 344–354, https://doi.org/10.1016/j.jtice.2016.11.014.

[2] S.A. Jafar, A.A. Aabid, J.I. Humadi, Corrosion behavior of carbon steel in 1 M, 2 M, and 3 M HCl solutions, Mater. Today Proc. (2021) 2–7, https://doi.org/10.1016/j.matpr.2021.12.295.

[3] Q.H. Zhang, Y.Y. Li, Y. Lei, X. Wang, H.F. Liu, G.A. Zhang, Comparison of the synergistic inhibition mechanism of two eco-friendly amino acids combined corrosion inhibitors for carbon steel pipelines in oil and gas production, Appl. Surf. Sci. 583 (2022), https://doi.org/10.1016/j.apsusc.2022.152559.

[4] F. Ríos, M. Lechuga, M. Fernández-Serrano, A. Fernández-Arteaga, Aerobic biodegradation of amphoteric amine-oxide-based surfactants: effect of molecular structure, initial surfactant concentration and pH, Chemosphere 171 (2017) 324–331, https://doi.org/10.1016/j.chemosphere.2016.12.070.

[5] T.D. Prichard, R.R. Thomas, C.M. Kausch, B.D. Vogt, Solubility of non-ionic poly (fluorooxetane)-block-(ethylene oxide)-block-(fluorooxetane) surfactants in carbon dioxide, J. Supercrit. Fluids 57 (2011) 95–100, https://doi.org/10.1016/j.supflu.2011.02.014.

[6] G. Wang, S. Wang, Z. Sun, S. Zheng, Y. Xi, Structures of nonionic surfactant modified montmorillonites and their enhanced adsorption capacities towards a cationic organic dye, Appl. Clay Sci. 148 (2017) 1–10, https://doi.org/10.1016/j.clay.2017.08.001.

[7] S. Cao, D. Liu, H. Ding, J. Wang, H. Lu, J. Gui, Task-specific ionic liquids as corrosion inhibitors on carbon steel in 0.5 M HCl solution: an experimental and theoretical study, Corros. Sci. 153 (2019) 301–313, https://doi.org/10.1016/j.corsci.2019.03.035.

[8] P. Kannan, J. Karthikeyan, P. Murugan, T.S. Rao, N. Rajendran, Corrosion Inhibition effect of novel methyl benzimidazolium Ionic liquid for carbon steel in HCl medium, J. Mol. Liq. 221 (2016) 368–380, https://doi.org/10.1016/j.molliq.2016.04.130.

[9] T. Douadi, H. Hamani, D. Daoud, M. Al-Noaimi, S. Chafaa, Effect of temperature and hydrodynamic conditions on corrosion inhibition of an azomethine compounds for mild steel in 1 M HCl solution, J. Taiwan Inst. Chem. Eng. 71 (2017) 388–404, https://doi.org/10.1016/j.jtice.2016.11.026.

[10] O. Kaczerewska, B. Brycki, I. Ribosa, F. Comelles, M.T. Garcia, Cationic gemini surfactants containing an O-substituted spacer and hydroxyethyl moiety in the polar heads: self-assembly, biodegradability and aquatic toxicity, J. Ind. Eng. Chem. 59 (2018) 141–148, https://doi.org/10.1016/j.jiec.2017.10.018.

[11] M. Mobin, R. Aslam, J. Aslam, Non toxic biodegradable cationic gemini surfactants as novel corrosion inhibitor for mild steel in hydrochloric acid medium and synergistic effect of sodium salicylate: Experimental and theoretical approach, Mater. Chem. Phys. 191 (2017) 151–167, https://doi.org/10.1016/j.matchemphys.2017.01.037.

[12] F.E.T. Heakal, A.E. Elkholy, Gemini surfactants as corrosion inhibitors for carbon steel, J. Mol. Liq. 230 (2017) 395–407, https://doi.org/10.1016/j.molliq.2017.01.047.

[13] Y. Zhang, Y. Pan, P. Li, X. Zeng, B. Guo, J. Pan, L. Hou, X. Yin, Novel Schiff base-based cationic Gemini surfactants as corrosion inhibitors for Q235 carbon steel and printed circuit boards, Colloids Surf. A Physicochem. Eng. Asp. 623 (2021), 126717, https://doi.org/10.1016/j.colsurfa.2021.126717.

[14] A.S. El-Tabei, A.E. El-Tabey, N.M.El Basiony, Newly imine-azo dicationic amphiphilic for corrosion and sulfate-reducing bacteria inhibition in petroleum processes: laboratory and theoretical studies, Appl. Surf. Sci. 573 (2022), https://doi.org/10.1016/j.apsusc.2021.151531.

[15] R. Zhang, J. Huo, Z. Peng, Q. Feng, J. Zhang, J. Wang, Emulsification properties of comb-shaped trimeric nonionic surfactant for high temperature drilling fluids based on water in oil, Colloids Surf. A Physicochem. Eng. Asp. 520 (2017) 855–863, https://doi.org/10.1016/j.colsurfa.2017.01.017.

[16] N.M. El Basiony, E.E. Badr, S.A. Baker, A.S. El-Tabei, Experimental and theoretical (DFT&MC) studies for the adsorption of the synthesized Gemini cationic surfactant based on hydrazide moiety as X-65 steel acid corrosion inhibitor, Appl. Surf. Sci. 539 (2021), 148246, https://doi.org/10.1016/j.apsusc.2020.148246.

[17] H. Ding, Y. Jiang, Y. Wang, H. Ju, T. Geng, Distributions of counterions on adsorption and aggregation behavior of Gemini quaternary ammonium salt, J. Mol. Liq. 342 (2021), 117495, https://doi.org/10.1016/j.molliq.2021.117495.

[18] M. Abdallah, M.A. Hegazy, M. Alfakeer, H. Ahmed, Adsorption and inhibition performance of the novel cationic gemini surfactant as a safe corrosion inhibitor for carbon steel in hydrochloric acid, Green Chem. Lett. Rev. 11 (2018) 457–468, https://doi.org/10.1080/17518253.2018.1526331.

[19] S.M. Shaban, S. Abd, S.M. Taw, A.A. Abdel-rahman, I. Aiad, Studying surface and thermodynamic behavior of a new multi-hydroxyl Gemini cationic surfactant and investigating their performance as corrosion inhibitor and biocide, J. Mol. Liq. 316 (2020), https://doi.org/10.1016/j.molliq.2020.113881.

[20] K.R. Ansari, D.S. Chauhan, M.A. Quraishi, T.A. Saleh, Surfactant modified graphene oxide as novel corrosion inhibitors for mild steels in acidic media, Inorg. Chem. Commun. 121 (2020), 108238, https://doi.org/10.1016/j.inoche.2020.108238.

[21] M.A. Hegazy, Novel cationic surfactant based on triazole as a corrosion inhibitor for carbon steel in phosphoric acid produced by dihydrate wet process, J. Mol. Liq. 208 (2015) 227–236, https://doi.org/10.1016/j.molliq.2015.04.042.

[22] A.S. Fouda, H.E. Megahed, N. Fouad, N.M. Elbahrawi, Corrosion inhibition of carbon steel in 1 M hydrochloric acid solution by aqueous extract of Thevetia peruviana, J. Bio- Tribo-Corros. 2 (2016) 1–13, https://doi.org/10.1007/s40735-016-0046-z.

[23] L. Huang, K.P. Yang, Q. Zhao, H.J. Li, J.Y. Wang, Y.C. Wu, Corrosion resistance and antibacterial activity of procyanidin B2 as a novel environment-friendly inhibitor for Q235 steel in 1 M HCl solution, Bioelectrochemistry 143 (2022), 107969, https://doi.org/10.1016/j.bioelechem.2021.107969.

[24] A.E. El-Tabey, A.G. Bedir, E.A. Khamis, M. Abd-El-Raouf, F. Zahran, M.A. Yousef, A.M. Al-Sabbagh, Synthesis and evaluation of new poly cationic surfactants as corrosion inhibitors for carbon steel in formation water, Egypt. J. Chem. 63 (2020) 833–850, https://doi.org/10.21608/ejchem.2019.11344.1730.

[25] S.M. Shaban, I. Aiad, M.M. El-Sukkary, E.A. Soliman, M.Y. El-Awady, Surface and biological activity of N-(((dimethoxybenzylidene)amino)propyl)-N,N-dimethylalkyl-1-ammonium derivatives as cationic surfactants, J. Mol. Liq. 207 (2015) 256–265, https://doi.org/10.1016/j.molliq.2015.03.043.

[26] M.A. Hegazy, S.S. Abd El-Rehim, E.A. Badr, W.M. Kamel, A.H. Youssif, Mono-, di- and tetra-cationic surfactants as carbon steel corrosion inhibitors, J. Surfactants Deterg. 18 (2015) 1033–1042, https://doi.org/10.1007/s11743-015-1727-1.
[27] E.a. Badr, H.H.H. Hefni, S.H. Shafek, S.M. Shaban, Synthesis of anionic chitosan surfactant and application in silver nanoparticles preparation and corrosion inhibition of steel, Int. J. Biol. Macromol. 157 (2020) 187–201.
[28] I. Aiad, M.M. El-Sukkary, A. El-Deeb, M.Y. El-Awady, S.M. Shaban, Surface properties, thermodynamic aspects and antimicrobial activity of some novel iminium surfactants, J. Surfactants Deterg. 15 (2012) 359–366.
[29] A.H. Tantawy, K.A. Soliman, H.M.Abd El-Lateef, Novel synthesized cationic surfactants based on natural Piper nigrum as sustainable-green inhibitors for steel pipeline corrosion in CO_2-3.5%NaCl: DFT, Monte Carlo simulations and experimental approaches, J. Clean. Prod. 250 (2020), 119510, https://doi.org/10.1016/j.jclepro.2019.119510.
[30] A.E. Fahim, R.M. Abdel Hameed, N.K. Allam, Synthesis and characterization of core-shell structured M@Pd/SnO2-graphene [M = Co, Ni or Cu] electrocatalysts for ethanol oxidation in alkaline solution, New J. Chem. 42 (2018) 6144–6160, https://doi.org/10.1039/c8nj01078a.
[31] N.M. El Basiony, A. Elgendy, A.E. El-Tabey, A.M. Al-Sabagh, G.M. Abd El-Hafez, M. A. El-raouf, M.A. Migahed, Synthesis, characterization, experimental and theoretical calculations (DFT and MC) of ethoxylated aminothiazole as inhibitor for X65 steel corrosion in highly aggressive acidic media, J. Mol. Liq. 297 (2020), 111940, https://doi.org/10.1016/j.molliq.2019.111940.
[32] S.M. Shaban, S.A. Elsamad, S.M. Tawfik, A.A.H. Abdel-Rahman, I. Aiad, Studying surface and thermodynamic behavior of a new multi-hydroxyl Gemini cationic surfactant and investigating their performance as corrosion inhibitor and biocide, J. Mol. Liq. 316 (2020), 113881, https://doi.org/10.1016/j.molliq.2020.113881.
[33] A.M. Al-Sabagh, M.A. Migahed, S.A. Sadeek, N.M.El Basiony, Inhibition of mild steel corrosion and calcium sulfate formation in highly saline synthetic water by a newly synthesized anionic carboxylated surfactant, Egypt. J. Pet. 27 (2018) 811–821, https://doi.org/10.1016/j.ejpe.2017.12.003.
[34] E.G. Zaki, T.A. Zidan, Methyl acrylate derivatives as corrosion inhibitors for X-65 type carbon steel in 1 M HCl, Int. J. Electrochem. Sci. 16 (2021), https://doi.org/10.20964/2021.03.23.
[35] M. Mobin, M. Parveen, Huda, R. Aslam, Effect of different additives, temperature, and immersion time on the inhibition behavior of L-valine for mild steel corrosion in 5% HCl solution, J. Phys. Chem. Solids 161 (2022), 110422, https://doi.org/10.1016/j.jpcs.2021.110422.
[36] M.A.M. El-Haddad, A. Bahgat Radwan, M.H. Sliem, W.M.I. Hassan, A.M. Abdullah, Highly efficient eco-friendly corrosion inhibitor for mild steel in 5 M HCl at elevated temperatures: experimental & molecular dynamics study, Sci. Rep. 9 (2019) 1–15, https://doi.org/10.1038/s41598-019-40149-w.
[37] M.M. Khalaf, A.H. Tantawy, K.A. Soliman, H.M.A. El-lateef, Cationic gemini-surfactants based on waste cooking oil as new ' green ' inhibitors for N80-steel corrosion in sulphuric acid: a combined empirical and theoretical approaches, J. Mol. Struct. 1203 (2020), 127442, https://doi.org/10.1016/j.molstruc.2019.127442.
[38] H.M.A. El-lateef, K. Shalabi, A.R. Sayed, S.M. Gomha, E.M. Bakir, The novel polythiadiazole polymer and its composite with a -Al (OH) 3 as inhibitors for steel alloy corrosion in molar H 2 SO 4: experimental and computational evaluations, J. Ind. Eng. Chem. 105 (2022) 238–250, https://doi.org/10.1016/j.jiec.2021.09.022.
[39] M.M. Saleh, M.G. Mahmoud, H.M.Abd El-Lateef, Comparative study of synergistic inhibition of mild steel and pure iron by 1-hexadecylpyridinium chloride and bromide ions, Corros. Sci. 154 (2019) 70–79, https://doi.org/10.1016/j.corsci.2019.03.048.
[40] H.M. Abd El-Lateef, K. Shalabi, A.H. Tantawy, Corrosion inhibition and adsorption features of novel bioactive cationic surfactants bearing benzenesulphonamide on C1018-steel under sweet conditions: combined modeling and experimental approaches, J. Mol. Liq. 320 (2020), 114564, https://doi.org/10.1016/j.molliq.2020.114564.
[41] R. Yildiz, A. Döner, T. Doğan, I. Dehri, Experimental studies of 2-pyridinecarbonitrile as corrosion inhibitor for mild steel in hydrochloric acid solution, Corros. Sci. 82 (2014) 125–132, https://doi.org/10.1016/j.corsci.2014.01.008.
[42] A. Döner, G. Kardaş, N-Aminorhodanine as an effective corrosion inhibitor for mild steel in 0.5M H2SO4, Corros. Sci. 53 (2011) 4223–4232, https://doi.org/10.1016/j.corsci.2011.08.032.
[43] S.A. Haddadi, E. Alibakhshi, G. Bahlakeh, B. Ramezanzadeh, M. Mahdavian, A detailed atomic level computational and electrochemical exploration of the Juglans regia green fruit shell extract as a sustainable and highly efficient green corrosion inhibitor for mild steel in 3.5 wt% NaCl solution, J. Mol. Liq. 284 (2019) 682–699, https://doi.org/10.1016/j.molliq.2019.04.045.
[44] R. Aslam, M. Mobin, J. Aslam, H. Lgaz, I.M. Chung, Inhibitory effect of sodium carboxymethylcellulose and synergistic biodegradable gemini surfactants as effective inhibitors for MS corrosion in 1 M HCl, J. Mater. Res. Technol. 8 (2019) 4521–4533, https://doi.org/10.1016/j.jmrt.2019.07.065.
[45] M. Mobin, R. Aslam, Experimental and theoretical study on corrosion inhibition performance of environmentally benign non-ionic surfactants for mild steel in 3.5% NaCl solution, Process Saf. Environ. Prot. 114 (2018) 279–295, https://doi.org/10.1016/j.psep.2018.01.001.
[46] K. Boumhara, M. Tabyaoui, C. Jama, F. Bentiss, Artemisia Mesatlantica essential oil as green inhibitor for carbon steel corrosion in 1 M HCl solution: Electrochemical and XPS investigations, J. Ind. Eng. Chem. 29 (2015) 146–155, https://doi.org/10.1016/j.jiec.2015.03.028.
[47] H.M. Abd El-Lateef, K. Shalabi, A.H. Tantawy, Corrosion inhibition of carbon steel in hydrochloric acid solution using newly synthesized urea-based cationic fluorosurfactants: experimental and computational investigations, New J. Chem. 44 (2020) 17791–17814, https://doi.org/10.1039/d0nj04004e.
[48] A.O. Alnajjar, H.M. Abd El-Lateef, M.M. Khalaf, I.M.A. Mohamed, Steel protection in acidified 3.5% NaCl by novel hybrid composite of CoCrO3/polyaniline: chemical fabrication, physicochemical properties, and corrosion inhibition performance, Constr. Build. Mater. 317 (2022), 125918, https://doi.org/10.1016/j.conbuildmat.2021.125918.
[49] H. Zhu, X. Li, X. Lu, J. Wang, Z. Hu, X. Ma, Efficiency of Gemini surfactant containing semi-rigid spacer as microbial corrosion inhibitor for carbon steel in simulated seawater, Bioelectrochemistry 140 (2021), 107809, https://doi.org/10.1016/j.bioelechem.2021.107809.
[50] M.A. Migahed, A. Nasser, H. Elfeky, M.M. El-Rabiei, The synthesis and characterization of benzotriazole-based cationic surfactants and the evaluation of their corrosion inhibition efficiency on copper in seawater, RSC Adv. 9 (2019) 27069–27082, https://doi.org/10.1039/c9ra04461b.
[51] D. Wang, Y. Li, B. Chen, L. Zhang, Novel surfactants as green corrosion inhibitors for mild steel in 15% HCl: Experimental and theoretical studies, Chem. Eng. J. 402 (2020), 126219, https://doi.org/10.1016/j.cej.2020.126219.
[52] J.M. Roque, T. Pandiyan, J. Cruz, E. García-Ochoa, DFT and electrochemical studies of tris(benzimidazole-2-ylmethyl)amine as an efficient corrosion inhibitor for carbon steel surface, Corros. Sci. 50 (2008) 614–624, https://doi.org/10.1016/j.corsci.2007.11.012.
[53] X. Jin, J. Wang, S. Zheng, J. Li, X. Ma, L. Feng, H. Zhu, Z. Hu, The study of surface activity and anti-corrosion of novel surfactants for carbon steel in 1 M HCl, J. Mol. Liq. 353 (2022), 118747, https://doi.org/10.1016/j.molliq.2022.118747.
[54] B. Sargolzaei, A. Arab, Synergism of CTAB and NLS surfactants on the corrosion inhibition of mild steel in sodium chloride solution, Mater. Today Commun. 29 (2021), 102809, https://doi.org/10.1016/j.mtcomm.2021.102809.
[55] S.A. Haladu, N. Dalhat Mu'azu, S.A. Ali, A.M. Elsharif, N.A. Odewunmi, H.M. Abd El-Lateef, Inhibition of mild steel corrosion in 1 M H2SO4 by a gemini surfactant 1,6-hexyldiyl-bis-(dimethyldodecylammonium bromide): ANN, RSM predictive modeling, quantum chemical and MD simulation studies, J. Mol. Liq. 350 (2022), 118533, https://doi.org/10.1016/j.molliq.2022.118533.
[56] P. Han, B. Zhang, Z. Chang, J. Fan, F. Du, C. Xu, R. Liu, L. Fan, The anticorrosion of surfactants toward L245 steel in acid corrosion solution: experimental and theoretical calculation, J. Mol. Liq. 348 (2022), 118044, https://doi.org/10.1016/j.molliq.2021.118044.
[57] R. Solmaz, G. Kardaş, M. Çulha, B. Yazici, M. Erbil, Investigation of adsorption and inhibitive effect of 2-mercaptothiazoline on corrosion of mild steel in hydrochloric acid media, Electrochim. Acta 53 (2008) 5941–5952, https://doi.org/10.1016/j.electacta.2008.03.055.
[58] H.M.A. Gouda, M. Khalaf, M.M. Shalabi, K. Al-Omair, M. A, El-Lateef, Synthesis and characterization of Zn – organic frameworks containing chitosan as a low-cost inhibitor for, Polymers 14 (2022) 228.
[59] H.M. Abd El-Lateef, A.H. Tantawy, A.A. Abdelhamid, Novel quaternary ammonium-based cationic surfactants: synthesis, surface activity and evaluation as corrosion inhibitors for C1018 carbon steel in acidic chloride solution, J. Surfactants Deterg. 20 (2017) 735–753, https://doi.org/10.1007/s11743-017-1947-7.
[60] H.M. Abd El-Lateef, H.S. El-Beltagi, M.E. Mohamed Mohamed, M. Kandeel, E. Bakir, A. Toghan, K. Shalabi, A.H. Tantawy, M.M. Khalaf, Novel natural surfactant-based fatty acids and their corrosion-inhibitive characteristics for carbon steel-induced sweet corrosion: detailed practical and computational explorations, Front. Mater. 9 (2022) 1–18, https://doi.org/10.3389/fmats.2022.843438.
[61] F. Bentiss, C. Jama, B. Mernari, H. El Attari, L. El Kadi, M. Lebrini, M. Traisnel, M. Lagrenée, Corrosion control of mild steel using 3,5-bis(4-methoxyphenyl)-4-amino-1,2,4-triazole in normal hydrochloric acid medium, Corros. Sci. 51 (2009) 1628–1635, https://doi.org/10.1016/j.corsci.2009.04.009.
[62] F. Bentiss, F. Gassama, D. Barbry, L. Gengembre, H. Vezin, M. Lagrenée, M. Traisnel, Enhanced corrosion resistance of mild steel in molar hydrochloric acid solution by 1,4-bis(2-pyridyl)-5H-pyridazino[4,5-b]indole: electrochemical, theoretical and XPS studies, Appl. Surf. Sci. 252 (2006) 2684–2691, https://doi.org/10.1016/j.apsusc.2005.03.231.
[63] F.M. Mahgoub, B.A. Abdel-Nabey, Y.A. El-Samadisy, Adopting a multipurpose inhibitor to control corrosion of ferrous alloys in cooling water systems, Mater. Chem. Phys. 120 (2010) 104–108, https://doi.org/10.1016/j.matchemphys.2009.10.028.
[64] A.G. Bedir, M. Abd El-Raouf, S. Abdel-Mawgoud, N.A. Negm, N.M.El Basiony, Corrosion inhibition of carbon steel in hydrochloric acid solution using ethoxylated nonionic surfactants based on schiff base: electrochemical and computational investigations, ACS Omega 6 (2021) 4300–4312, https://doi.org/10.1021/acsomega.0c05476.
[65] S.M. Shaban, R.M. El-Sherif, M.A. Fahim, Studying the surface behavior of some prepared free hydroxyl cationic amphipathic compounds in aqueous solution and their biological activity, J. Mol. Liq. 252 (2018) 40–51.
[66] S.M. Tawfik, Ionic liquids based gemini cationic surfactants as corrosion inhibitors for carbon steel in hydrochloric acid solution, J. Mol. Liq. 216 (2016) 624–635, https://doi.org/10.1016/j.molliq.2016.01.066.
[67] A.S. El-Tabei, M.A. Hegazy, A.H. Bedair, N.M. El Basiony, M.A. Sadeq, Novel macrocyclic cationic surfactants: Synthesis, experimental and theoretical studies of their corrosion inhibition activity for carbon steel and their antimicrobial activities, J. Mol. Liq. 345 (2022), 116990, https://doi.org/10.1016/j.molliq.2021.116990.

[68] S.S.A. El, R.S.M. Sayyah, S.M. Kamal, Adsorption and corrosion inhibitive properties of P (2-aminobenzothiazole) on mild steel in hydrochloric acid media, Int. J. Ind. Chem. 7 (2016) 39–52, https://doi.org/10.1007/s40090-015-0065-5.
[69] F. Zhang, Y. Tang, Z. Cao, W. Jing, Z. Wu, Y. Chen, Performance and theoretical study on corrosion inhibition of 2-(4-pyridyl)-benzimidazole for mild steel in hydrochloric acid, Corros. Sci. 61 (2012) 1–9, https://doi.org/10.1016/j.corsci.2012.03.045.
[70] C. Wang, C. Zou, Y. Cao, Electrochemical and isothermal adsorption studies on corrosion inhibition performance of β-cyclodextrin grafted polyacrylamide for X80 steel in oil and gas production, J. Mol. Struct. 1228 (2021), 129737, https://doi.org/10.1016/j.molstruc.2020.129737.
[71] M. Abdallah, H.M. Eltass, M.A. Hegazy, H. Ahmed, Adsorption and inhibition effect of novel cationic surfactant for pipelines carbon steel in acidic solution, Prot. Met. Phys. Chem. Surf. 52 (2016) 721–730, https://doi.org/10.1134/S207020511604002X.
[72] M. El Faydy, R. Touir, M. Ebn Touhami, A. Zarrouk, C. Jama, B. Lakhrissi, L. O. Olasunkanmi, E.E. Ebenso, F. Bentiss, Corrosion inhibition performance of newly synthesized 5-alkoxymethyl-8-hydroxyquinoline derivatives for carbon steel in 1 M HCl solution: experimental, DFT and Monte Carlo simulation studies, Phys. Chem. Chem. Phys. 20 (2018) 20167–20187, https://doi.org/10.1039/c8cp03226b.
[73] S.M. Shaban, I. Aiad, M.M. El-Sukkary, E.A. Soliman, M.Y. El-Awady, Evaluation of some cationic surfactants based on dimethylaminopropylamine as corrosion inhibitors, J. Ind. Eng. Chem. 21 (2015) 1029–1038, https://doi.org/10.1016/j.jiec.2014.05.012.
[74] M.A. Gebril, M.A. Bedair, S.A. Soliman, M.F. Bakr, M.B.I. Mohamed, Experimental and computational studies of the influence of non-ionic surfactants with coumarin moiety as corrosion inhibitors for carbon steel in 1.0 M HCl, J. Mol. Liq. 349 (2022), 118445, https://doi.org/10.1016/j.molliq.2021.118445.
[75] G. Xia, X. Jiang, L. Zhou, Y. Liao, M. Duan, H. Wang, Q. Pu, J. Zhou, Enhanced anticorrosion of methyl acrylate by covalent bonded N-alkylpyridinium bromide for X70 steel in 5M HCl, J. Ind. Eng. Chem. 27 (2015) 133–148, https://doi.org/10.1016/j.jiec.2014.12.027.
[76] M.M. Salim, M.M. Azab, M.A. Abo-Riya, M. Abd-El-Raouf, N.M.E.L. Basiony, Controlling C-steel dissolution in 1M HCl solution using newly synthesized ρ-substituted imine derivatives: theoretical (DFT and MCs) and experimental investigations, J. Mol. Struct. (2022), 134357.
[77] A.M. Al-Sabagh, N.M. El Basiony, S.A. Sadeek, M.A. Migahed, Scale and corrosion inhibition performance of the newly synthesized anionic surfactant in desalination plants: experimental, and theoretical investigations, Desalination 437 (2018) 45–58, https://doi.org/10.1016/j.desal.2018.01.036.
[78] A.S. El-Tabei, O.E. El-Azabawy, N.M. El Basiony, M.A. Hegazy, Newly synthesized quaternary ammonium bis-cationic surfactant utilized for mitigation of carbon steel acidic corrosion; theoretical and experimental investigations, J. Mol. Struct. 1262 (2022), 133063, https://doi.org/10.1016/j.molstruc.2022.133063.
[79] L.O. Olasunkanmi, I.B. Obot, M.M. Kabanda, E.E. Ebenso, Some quinoxalin-6-yl derivatives as corrosion inhibitors for mild steel in hydrochloric acid: experimental and theoretical studies, J. Phys. Chem. C 119 (2015) 16004–16019, https://doi.org/10.1021/acs.jpcc.5b03285.
[80] I. Nadi, M. Bouanis, F. Benhiba, K. Nohair, A. Nyassi, A. Zarrouk, C. Jama, F. Bentiss, Insights into the inhibition mechanism of 2,5-bis(4-pyridyl)-1,3,4-oxadiazole for carbon steel corrosion in hydrochloric acid pickling via experimental and computational approaches, J. Mol. Liq. 342 (2021), 116958, https://doi.org/10.1016/j.molliq.2021.116958.
[81] M. El Faydy, F. Benhiba, I. Warad, H. About, S. Saoiabi, A. Guenbour, F. Bentiss, B. Lakhrissi, A. Zarrouk, Experimental and theoretical investigations of two quinolin-8-ol derivatives as inhibitors for carbon steel in 1 M HCl solution, J. Phys. Chem. Solids 165 (2022), 110699, https://doi.org/10.1016/j.jpcs.2022.110699.
[82] M. El Faydy, F. Benhiba, I. Warad, A.S. Abousalem, H. About, Y. Kerroum, C. Jama, A. Guenbour, B. Lakhrissi, A. Zarrouk, Appraisal of corrosion inhibiting ability of new 5-N-((alkylamino)methyl)quinolin-8-ol analogs for C40E steel in sulfuric acid, Int. J. Hydrog. Energy 46 (2021) 30246–30266, https://doi.org/10.1016/j.ijhydene.2021.06.205.
[83] M.H. Sliem, M. Afifi, A.B. Radwan, E.M. Fayyad, M.F. Shibl, F.E. Heakal, M. A. Aboubakr, AEO7 surfactant as an eco-friendly corrosion inhibitor for carbon steel in HCl solution, Sci. Rep. (2019) 1–16, https://doi.org/10.1038/s41598-018-37254-7.
[84] B.F. Zehra, A. Said, H.M. Eddine, E. Hamid, H. Najat, N. Rachid, L.I. Toumert, Crataegus oxyacantha leaves extract for carbon steel protection against corrosion in 1M HCl: characterization, electrochemical, theoretical research, and surface analysis, J. Mol. Struct. 1259 (2022), 132737, https://doi.org/10.1016/j.molstruc.2022.132737.
[85] S.A. Umoren, R.K. Suleiman, I.B. Obot, M.M. Solomon, A.Y. Adesina, Elucidation of corrosion inhibition property of compounds isolated from Butanolic Date Palm Leaves extract for low carbon steel in 15% HCl solution: experimental and theoretical approaches, J. Mol. Liq. 356 (2022), 119002, https://doi.org/10.1016/j.molliq.2022.119002.